Master Thesis in Geosciences

Comparison of Hydrological Impacts of Climate Change Simulated by WASMOD and HBV Models in Different Climatic Zones

China, Ethiopia, and Norway

Eregno, Fasil Ejigu

UNIVERSITY OF OSLO

FACULTY OF MATHEMATICS AND NATURAL SCIENCES

Comparison of Hydrological Impacts of Climate Change Simulated by WASMOD and HBV Models in Different Climatic Zones

China, Ethiopia, and Norway

Eregno, Fasil Ejigu

Master Thesis in Geosciences

Discipline: Hydrology

Department of Geosciences

Faculty of Mathematics and Natural Sciences

UNIVERSITY OF OSLO

June, 2009

Table of Contents

List of Figures

List of Tables

Acronyms

IPCC	Intergovernmental Panel on Climate Change
WASMOD	Water And Snow balance MODeling system
HBV	Hydrologiska Byråns Vettenbalansavdelning
	(Hydrological bureau water balance section)
NVE	Norges Vassdrags og Energidirektorat
	(Norwegian Water Resource and Energy Directorate)
DEM	Digital Elevation Model
SRTM	Shuttle Radar Topography Mission
ENMA	Ethiopian National Meteorology Agency
GCM	General Circulation Model
RCM	Regional Circulation Model
TGICA	Task Group on data and scenario support for Impact and Climate Assessment
E	Nash–Sutcliffe model efficiency coefficient
RMSE	Root Mean Square Error
RVE	Relative Volume Error
ΔP	Change in Precipitation
ΔT	Change in Temperature

Acknowledgments

I would like to express my gratitude to the department of Geosciences, my host institute for granting me field work expenses to peruse this study.

I am grateful to Professor Chong-Yu Xu, my supervisor, for his invaluable comments and continuous guidance throughout the study. I am also grateful to Mr. Diress Tsegaye, who provides to me valuable comments when I write the thesis.

My gratitude also goes to Ministry of Water Resource and National meteorology Agency of Ethiopia for their collaboration in providing meteorological and stream flow data. I also thank Norwegian Water Resource and Energy Directorate (NVE) for providing stream flow data and study area digital maps.

Special and heartfelt appreciation goes to my wife, Mebrat Gebreslassie, who had always been with me when I need help more than ever. I am grateful for her comments and assistance during my study. I would like to thank my parents and friends for their continuous encouragement during my study.

Dedication

This thesis is dedicated to my wife, Mebrat Gebreslasie who is a corner stone of our family.

Abstract

Recent advances in hydrological impact studies points that the response of specific catchments to climate change scenario using a single model approach is questionable. Based on this hypothesis, this study was aimed at investigating the impact of climate change on the hydrological regime of river basins in three different climatic zones (China, Ethiopia and Norway) using WASMOD and HBV hydrological models. Specifically the objectives include (i) examining and comparing the hydrological response of different river basins to climate change scenarios, (ii) testing the sensitivity of WASMOD and HBV models, and (iii) testing the sensitivity of climate change scenarios in different climatic regions. The climate change response of the three basins (Didessa, Dongjiang and Elverum) were evaluated in terms of runoff, actual evapotranspiration and soil moisture storage change for incremental precipitation and temperature change scenarios using HBV and WAMOD models. The parameters of hydrological models were determined in the study catchment using current climatic inputs and observed river flows. The historical time series of climatic data was adjusted according to the climate change scenarios. The hydrological characteristics of the catchments under the adjusted climatic conditions were simulated using the calibrated hydrological model. Finally, comparisons of the model simulations of the current and possible future hydrological characteristics were performed. The calibration and validation results of WASMOD and HBV models show that both models can reproduce the runoff with acceptable accuracy for each basin. The findings of this study demonstrated that high sensitivity was observed for Didessa and Elverum to precipitation and temperature changes, respectively. However, Dongjiang was found less sensitive to both precipitation and temperature changes. In general, the results imply that there is limitation in moisture and temperature for Didessa and Elverum, respectively. The hydrological impact of climate

change resulted from synthetic scenario using the two models indicate that the sensitivity of catchments in response to different climate change scenario was different in different climatic regions. Thus, the result demonstrated a concern that hydrological impact of climate change analysis using single hydrological model may lead to unreliable conclusion. In this regard, conducting multi model analysis is one way to reduce such uncertainty. Finally, we recommend further research in this area in order to exhaustively explore hydrological impact of climate change in different regions.

1. Introduction

1.1 Background Information

Climate change refers to the change in the state of the mean and/or variability of climate properties over time, due to natural variability or as a result of anthropogenic activity (IPCC, 2007). The anthropogenic production of greenhouse gases will induce many changes in the natural environment. The most obvious of these are on the climate, through increasing mean global temperatures, modifying precipitation distributions and change evapotranspiration rate (Karl, 1996). Nowadays there is strong scientific evidence that the average temperature of the Earth's surface is increasing due to greenhouse gas emissions and predicted that mean surface temperatures may rise 0.3–0.6^{o}C per decade in the 21st century (IPCC, 2001).

With respect to hydrology, climate change can cause significant impacts on water resources by resulting changes in the hydrological cycle. The increasing trend of temperature will lead to greater amounts of water vapour in the atmosphere and the hydrological cycle will be intensified with more precipitation. However, the extra precipitation will be unequally distributed around the globe. Some parts of the world may see significant reductions in precipitation, or alterations in the timing of wet and dry seasons and would lead to increases in both floods and droughts (Seino et al., 1998). The spatial change in amount, intensity and frequency of the precipitation will affect the magnitude and frequency of river flows; consequently, it will substantially affect the water resources at local and regional levels.

Climate change is expected to have adverse impacts on socioeconomic development in all nations and the degree of the impact will differ. Such hydrologic changes will affect nearly every aspect of human well-being, from agricultural productivity and energy use to flood control, municipal and industrial water supply, and fish and wildlife management (Xu,

2000). The tremendous importance of water in both society and nature underscores the necessity of understanding how a change in global climate could affect regional water supplies and it has motivated many researchers to conduct studies using different approaches. In this regard, quantitative estimates of the hydrological effects of climate change at local and regional scales are essential for understanding and solving the potential water resource management problems associated with water supply for domestic and industrial water use, power generation, and agriculture (Steele-Dunne et al., 2008). Therefore, the ability to understand the hydrologic response of climate change will help policy makers to guide planning and form more resilient infrastructure in the future.

Hydrological models provide a framework to conceptualise and investigate the relationships between climate, and water resources (Jothityangkoon et al., 2001). The three most often used classification of hydrological models are; empirical or black-box, conceptual or grey-box, and physically based distributed or white-box models. Empirical models do not explicitly consider the governing physical laws of the process involved, but only relate input to output through some transform function. Conceptual models consider physical laws but in highly simplified form and represent the effective response of an entire catchment, without attempting to characterise the spatial variability of the response explicitly. Physically based distributed models contain parameters that have concurrent measurements of physical significance and explicitly represent the spatial variability of most of the important land surface characteristics (Xu, 2006).

Many studies of the impact of climate change on the hydrology of specific geographic regions with single hydrological model have been reported (Beldring et al., 2008; Christensen et al., 2004; Jha et al., 2006; Steele-Dunne et al., 2008; Xu, 2000). When multi models are used to investigate the hydrological impact of climate change, big differences

exist in model prediction depend on the climate scenarios, the season, and the hydrological variables under examination (Jiang et al, 2007). Therefore, they warn that future water resources scenarios predicted by any particular hydrological model represent only the results of that model, and strongly recommend that more studies using different hydrological models on different climatic regions need to be carried out in order to provide more general conclusions. This study attempts to place the hydrological consequences of climate change in three different climate zones using two hydrological models and provide complete depiction in order to provide more general conclusions as recommend more studies using different hydrological models on different catchments (Jiang et al., 2007). The two models used to investigate the hydrological impact of climate change have been used widely in different climatic regions. They are HBV-light, daily water balance model described in (Seibert. J., 1998) and WASMOD, monthly water balance model described in (Xu, 2002). The potential of the models for studies of climate change impact on hydrological regimes of river basins is presented (Beldring et al., 2008; Steele-Dunne et al., 2008; Xu, 2000).

1.2 Objectives of the study

This study is aimed at investigating the impact of climate change on the hydrological regime of river basins in three different climatic zones using WASMOD and HBV hydrological models. Specifically the objectives are:

- To examine and compare the hydrological response of different climatic zones river basin's to different climate change scenarios.
- To test the sensitivity of WASMOD and HBV models for climate change scenarios in different climatic regions
- To test the sensitivity of different climate change scenarios in different climatic regions using two hydrological models.

2. Study areas and data

2.1 Dongjiang Basin (China)

Dongjiang basin is one of the Zhujiang sub-basins located in Guangdong and Jiangxi provinces in southern China (Figure 1). The drainage area of the river basin is 25,555 Km^2 and flows from north-east to south-west direction. The landscape of the basin is characterized by hills which account 78.1 % and the remaining 14.4 % is plains (Jin et al., 2008). Dongjiang basin has sub-tropical climate with the mean annual temperature of 21^oC and average annual rainfall of 1747 mm for the period 1960 – 1988. Frontal and typhoon type of storms are the most common type of rainfalls which generate precipitation for the basin. The temperature of the basin occasionally dropped below 0^oC in the mountains of the upstream area during the winter time (Jiang et al., 2007). In this study, areal rainfall was calculated from the records of the 51 stations using the Thiessen polygon method, mean daily temperature from 8 stations and evaporation data from 5 stations were organized in order to use as model input for the period of 1978 – 1988.

2.2 Didessa Basin (Ethiopia)

Didessa river basin is located in the South Western part of Ethiopia (Figure 1). The catchment area of the river basin encompasses approximately 9981 Km^2 up to the river gauge near Arjo as it is extracted a Shuttle Radar Topographic Mission (SRTM) Digital Elevation Model (DEM). Didessa river is a part of the upper Blue Nile drainage system and it covers around 5.4 % of the upper Blue Nile basin area and the river is the largest tributary of upper Blue Nile river which contributes 10.7 % of the total discharge (Conway, 2000).

Climate of the study area varies from humid to semiarid and most precipitation occurs in the wet season called Kiremt (May-September) which accounts 78 % of the annual precipitation.

The remaining precipitation occurs in the dry season from October to April, which accounts 22 % according to the 1985-1999 precipitation data. The primary climatic and hydrologic daily data set used for this study was obtained from Ethiopian National Meteorological Agency and Ministry of Water Resources respectively. The climatic data contain precipitation, temperature and evaporation, while the hydrological data contain river discharge. The rainfall data base of daily time series consisted of records from 10 rainfall stations with 7 time series covering the period from 1985 to 1999, while the remaining 3 started operation during 1987 – 1990. The model input of areal precipitation data was calculated using the Thiessen polygon method and the daily data were aggregated to create monthly data set.

2.3 Elverum Basin (Norway)

Elverum catchment is a part of Glomma basin and located in the south eastern part of Norway (Figure 1). The drainage area of the basin up to Elverum river gauge station is 15449 Km^2. The head waters are partially glacier-faced high mountains and drain downstream to south, Lake Mjosa, the largest lake in Norway. The upper head water is the catchment of Hummelvoll which is nested within Elverum. The basin is characterized by cold winter and relatively warm summer (the mean annual temperature at Hummelvoll is 0.3^oC and the mean annual precipitation ranges from 450 – 890 mm). The hydrology of the area is characterized by low flow during winter caused by snow accumulation and high flow during snow melt in spring or early summer (Henny A.J. van Lanen et al., 2008). All the hydro-climatic data consider in this study was acquired from Norwegian Water Resource and Energy Directorate (NVE). and from Norwegian Meteorological institute (eKlima) archive.

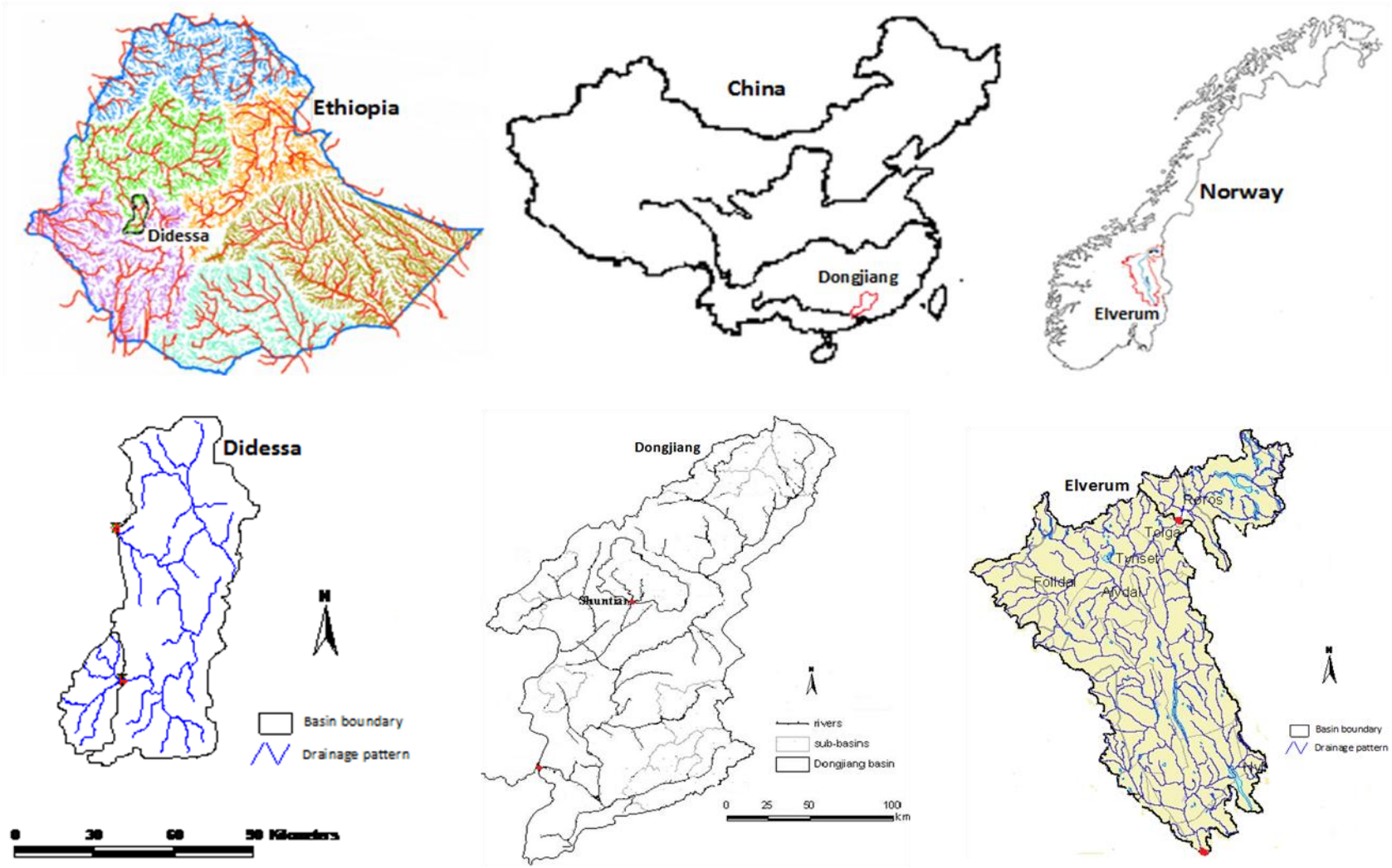

Figure 1. The catchment of Didessa, Dongjiang, and Elverum and their location Ethiopis, China, and Norway

3. Methodology

3.1 Approach

Research on hydrological impact of climate change is a three-step process essentially consists of: (1) producing global climate change scenarios by using general circulation models (GCMs) in association with increasing greenhouse gases, (2) producing regional and catchment scale climate change scenarios by using hypothetical method or downscaling techniques through which the GCM outputs are downscaled to the scales compatible with hydrological models, and (3) producing future water resources scenarios at regional and catchment scales by using hydrological models with regional and catchment scale climate change scenarios as input.

Such studies usually follow the four steps (Xu, 1999; Xu, 2005):

1. The parameters of hydrological models were determined in the study catchment using current climatic inputs and observed river flows for model calibration and validation.
2. The historical time series of climatic data was adjusted according to the climate change scenarios (hypothetical or downscaled).
3. The hydrological characteristics of the catchment under the adjusted climate were simulated using the calibrated hydrological model.
4. Comparisons of the model simulations of the current and possible future hydrological characteristics were performed

3.2 Climate Change Scenarios

The development of climate change scenarios is an important step in the hydrological impact of climate change study. A climate change scenario refers to a representation of the

difference between some plausible future climate and the current or control climate (IPCC, 2001). It is a probable indication of what the future could be like over decades or centuries, given a specific set of assumptions. A number of different methods exist to construct climate change scenarios that include techniques utilising climate analogues, synthetic scenarios, general circulation model (GCM) scenarios (Carter, 1995).

Analogue scenarios are constructed by identifying recorded climate regimes which may resemble the future climate in a given region. These records can be obtained either from the past (temporal analogues) or from another region at the present (spatial analogues) (IPCC-TGICA, 2007). Therefore, in analogues scenarios, spatially or temporally displaced climate data are used as climate change scenarios.

Arbitrary (Synthetic) scenarios describe techniques where particular climatic elements are changed by a realistic but arbitrary amount, often according to a qualitative interpretation of climate model simulations for a region. For example, adjustments of baseline temperatures by +1, +2, +3 and +4°C and baseline precipitation by ±5, ±10, ±15 and ±20 percent could represent various magnitudes of future change (IPCC-TGICA, 2007). For instance, this type of climate change scenario has been used to study the effects of climate change on water resources in central Sweden (Xu, 2000). The main advantages of synthetic scenarios are simple to apply, transparent and easily interpreted by policy makers and non-specialists. In addition, they capture a wide range of possible changes in climate, offering a useful tool for evaluating the sensitivity of an exposure unit to changing climate. Since individual variables can be altered independently of each other, synthetic scenarios also help to describe the relative sensitivities to changes in different climatic variables. Moreover, they can assist in identifying thresholds or discontinuities of response that might occur under a given

magnitude or rate of climate change. Different studies can readily apply the same synthetic scenarios to explore relative sensitivities of exposure units. This is potentially useful for comparing and synthesizing the potential effects of climate change over different sectors and regions (IPCC-TGICA, 2007).

General circulation models (GCMs) are sophisticated mathematically based simulations of the world's climate including atmospheric, oceanic, cryospheric, and land surface components (Gagnon and Gough, 2005). GCMs, often in conjunction with nested regional models or other downscaling methods, have the potential to provide geographically and physically consistent estimates of regional climate change which are required in impact analysis. However, their resolution is quite coarse relative to the scale of exposure units in most impact assessments. Given the limitations of GCMs grid-point predictions for regional climate change impact studies, an alternative option is to downscale GCM's climate output for use in hydrological models. Downscaling can be defined as a technique that allows increases the resolution of the Global Climate Models (GCMs regional scale) to obtain local scale surface weather for several applications (IPCC-TGICA, 2007).

In this study, we used only the hypothetical scenario in order to investigate the response of river basins in different climatic zone to climate change and the sensitivity of hydrological models (WASMOD and HBV) for the same climate change scenarios. In order to cover a wide range of climate variability, ten hypothetical climate change scenarios were derived from combinations of two absolute temperature changes and five relative precipitation changes (Table 1).

Table 1. Hypothetical climate change scenarios

Scenarios	**1**	**2**	**3**	**4**	**5**	**6**	**7**	**8**	**9**	**10**
ΔT (^{o}C)	2	2	2	2	2	4	4	4	4	4
ΔP (%)	-20	-10	0	+10	+20	-20	-10	0	+10	+20

3.3 Hydrological Models

Hydrologic models are simplified, conceptual representations of a part of the hydrologic cycle and predominantly used for hydrologic prediction and understanding of hydrologic processes (Dooge, 1977). Based on the description of the physical processes, hydrological models can be classified as conceptual model which consider physical laws but in highly simplified form, and physically based models which contain parameters that have concurrent measurements of physical significance. On the other hand, according to the spatial description of catchment processes, hydrological models can be categorized as lumped model, treating the complete basin as a homogeneous whole, and distributed model, the whole basin is divided into elementary unit areas like a grid net and flows are passed from one grid point (node) to another as water drains through the basin (Xu, 2006). For this study, WASMOD lumped conceptual hydrological model and HBV semi-distributed conceptual models are selected based on; (1) the nature of physical processes that interact to produce the phenomena under investigation, (2) availability of the required information, (3) widely applicability and popularity of the models, and (4) the acquaintance with the models.

3.3.1 HBV Model

HBV model was first developed at the Swedish Meteorological and Hydrological Institute (Bergstrom and Forsman, 1973). The HBV model is a water balance based mathematical model of the hydrological processes in a catchment used to simulate the runoff properties using rainfall, temperature and potential evaporation data. The model consists of different routines representing snow by a degree-day method, soil water and evaporation, groundwater by three linear reservoir equations and channel routing by a triangular weighting function (Seibert, 1997). The HBV model version used in this study is HBV light (Seibert, 2005) and the conceptualization of the model is shown in Fig 2 (Seibert. J., 1998).

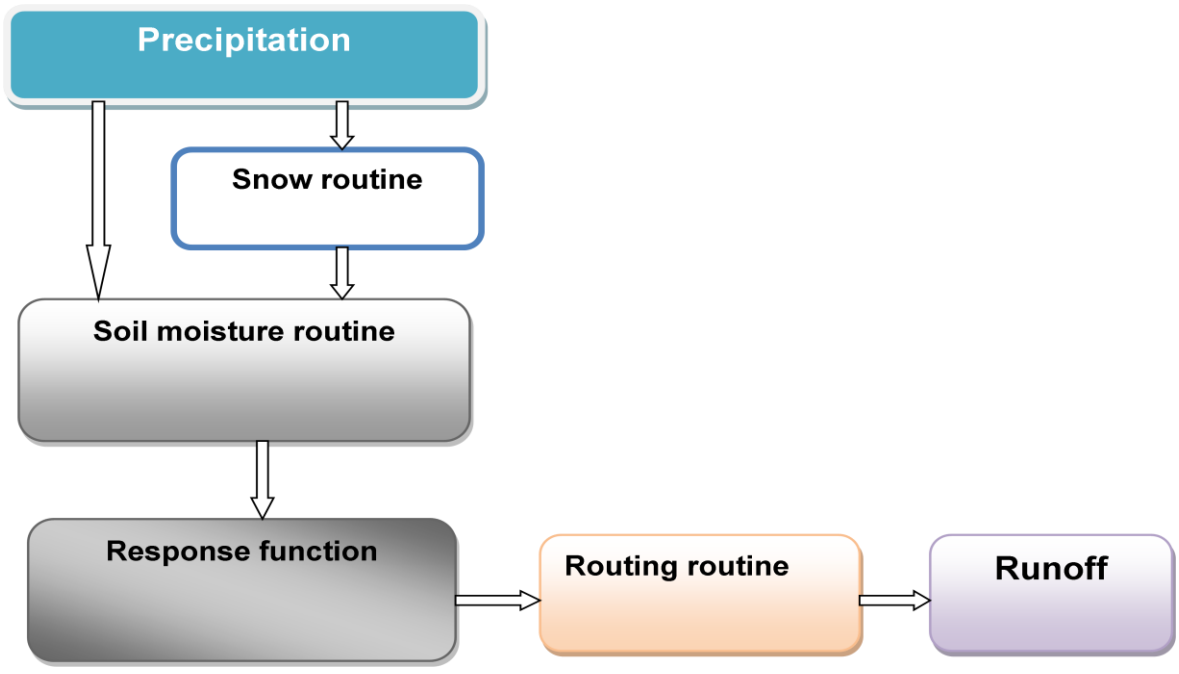

Figure 2. Schematic structure of HBV model

As described by Seibert (2005), the HBV model runs on daily time step to simulate daily discharge using daily rainfall, temperature and potential evaporation as inputs. Precipitation is simulated to be either snow if the temperature is below the threshold temperature TT (°C)

or rain if the temperature is above the threshold temperature, TT (°C). In order to represents systematic errors in the snowfall measurements and the 'missing' evaporation from the snow pack in the model, snowfall correction factor, SFCF (-) is multiplied by the precipitation simulated to be snow when the temperature is below TT. Snow melt is calculated with the degree-day method (Eq. (A1)). The snow pack retains melted water and rainfall until it exceeds a certain fraction, CWH (-), which is the water equivalent of the snow. Liquid water within the snow pack refreezes according to a refreezing coefficient, CFR (-) (Eq. (A2)).

$$Melt = CFMAX * (T(t) - TT) \quad \text{(A1)}$$

$$Refreezing = CFR * CFMAX * (TT - T(t)) \quad \text{(A2)}$$

Rainfall and snow melt (*P*) are divided into water filling the soil box and groundwater recharge depending on the relation between water content of the soil box (*SM* (mm)) and its largest value (FC (mm)) (Eq. (A3)). Actual evaporation from the soil box equals the potential evaporation if *SM*/FC is above LP (-), while a linear reduction is used when *SM*/FC is below LP (Eq. (A4)).

$$\frac{recharge}{p(t)} = \left[\frac{SM(t)}{FC} \right]^{BETA} \quad \text{(A3)}$$

$$E_{act} = E_{pot} * \min \left[\frac{SM(t)}{FC * LP}, 1 \right] \quad \text{(A4)}$$

Groundwater recharge is added to the upper groundwater box (*SUZ* (mm)). PERC (mm d^{-1}) defines the maximum percolation rate from the upper to the lower groundwater box (*SLZ* (mm)). For the lake area, precipitation and evaporation is added and subtracted directly from the lower box. Runoff from the groundwater boxes is computed as the sum of two or three linear outflow equations (K_0, K_1 and K_2 (d^{-1})) depending on whether *SUZ* is above a threshold value, UZL (mm), or not (Eq. (A5)). This runoff is finally transformed by a triangular

weighting function defined by the parameter MAXBAS (d) (Eq. (A6)) to give the simulated runoff (mm d^{-1}). The model has in total 10 parameters to be calibrated.

$$Q_{GW}(t) = K_2 * SLZ + K_1 * SUZ + K_0 * \max(SUZ - SLZ, 0) \quad \text{(A5)}$$

$$Q_{aim}(t) = \sum_{i=1}^{MAXBAS} C(i) * Q_{GW}(t - i + 1)$$
$$where, c(i) = \int_{i-1}^{i} \frac{2}{MAXBAS} - \left| u - \frac{MAXBAS}{2} \right| * \frac{4}{MAXBAS^2} du \quad \text{(A6)}$$

3.3.2 WASMOD model

The Water And Snow balance MODeling system (WASMOD) is a conceptual lumped modeling system. The model version used in this study was developed by (Xu, 2002). WASMOD is monthly water balance model that requires monthly values of areal precipitation, potential evapotranspiration and air temperature as inputs. The model outputs are monthly river flow and other water balance components, such as actual evapotranspiration, slow and fast components of river flow, soil-moisture storage and accumulation of snowpack. The schematic representation of WASMOD is given in Fig 3 (Xu, 2002).

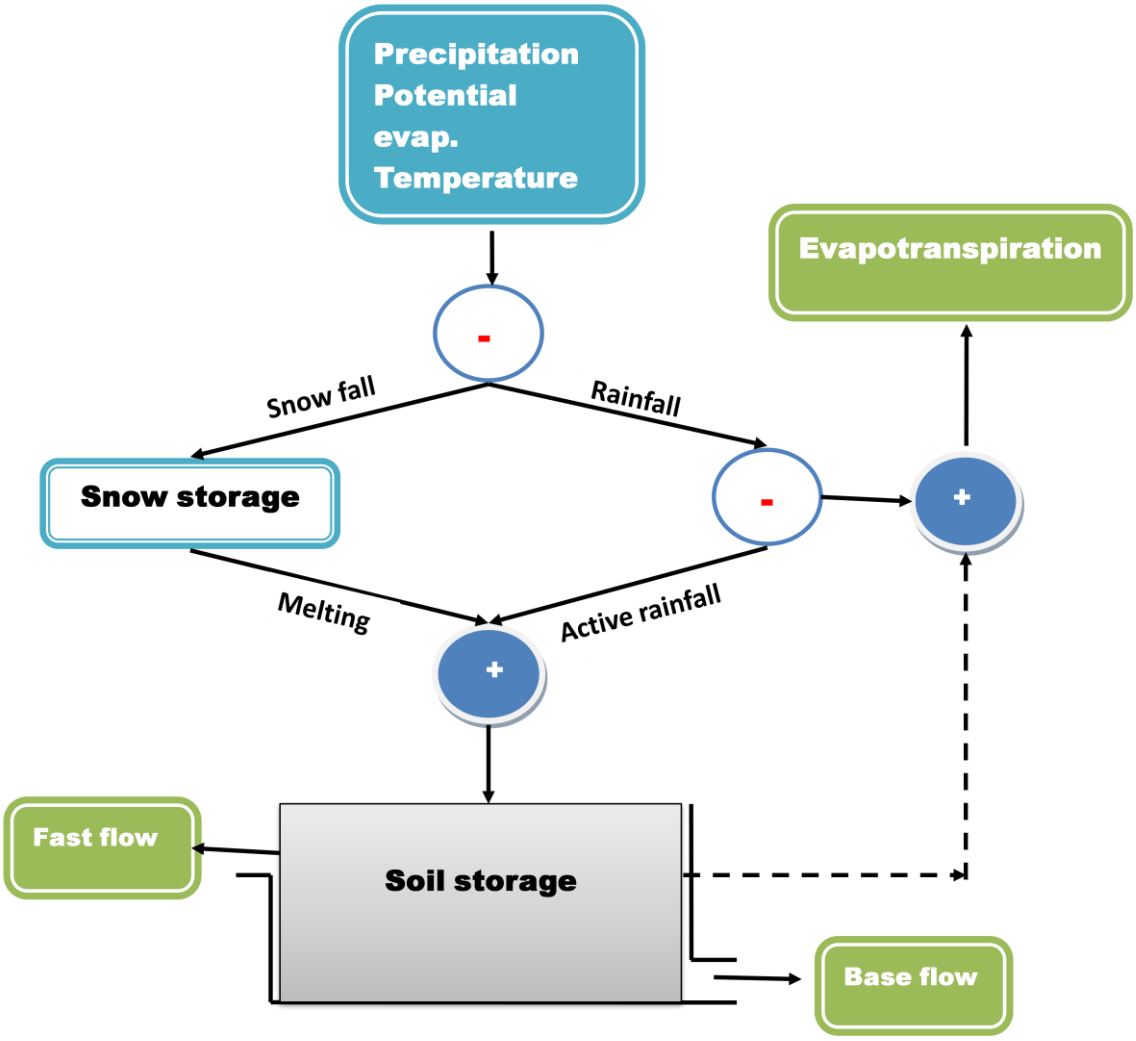

Figure 3. The concept of WASMOD model system

As the model described in (Xu, 2002), temperature-index function is used to separate rainfall r_t and snowfall s_t and then snowfall is added to the snowpack sp_t (the first storage) at the end of the month, of which a fraction m_t melts and contributes to the soil-moisture storage sm_t. Temperature-index method is used to calculated snowmelt. A part of rainfall is subtracted and added to interception evaporation loss before the rainfall contributes to the soil storage. The soil storage contributes to evapotranspiration e_t , to a fast component of flow f_t and to base flow b_t. All the above mentioned processes are governed by six parameters (a1 - a6) and the principal equations for the parameters are presented in Table 2 (Engeland et al., 2005). When

the model is applied to snow free catchments, only 3 parameters need to be calibrated which are controlling actual evapotranspiration, fast flow and slow flow, respectively.

Table 2 Principal equations for the parameters of WASMOD model

Snowfall	$s_t = p_t\{1 - \exp[-(ct - a)/(a_1 - a_2)]^2\}^+$	$a_1 \geq a_2$
Rainfall	$r_t = p_t - s_t$	
Snow storage	$sp_t = sp_{t-1} + s_t - m_t$	
Snowmelt	$mt = sp_t\{1 - \exp[-(c_t - a_2)/(a_1 - a_2)]^2\}^+$	
Potential evapotranspiration	$ept = [1 + a_3(c_t - c_m)]ep_m$	
Actual evapotranspiration	$et = \min\{w_t[1 - \exp(-a_4 ep_t)], ep_t\}$	$0 \leq a_4 \leq 1$
Slow flow	$b_t = a_5(sm^+_{t-1})^2$	$a_5 \geq 0$
Fast flow	$f_t = a_6(sm^+_{t-1})^2 (m_t + n_t)$	$a_6 \geq 0$
Water balance	$sm_t = sm_{t-1} + r_t + m_t - e_t - b_t - f_t$	

$w_t = r_t + sm^+_{t-1}$ is the available water; sm^+_{t-1} is the available storage; $n_t = r_t - ep_t(1 - \exp(r_t/ep_t))$ is the active rainfall; p_t and c_t are monthly precipitation and air temperature respectively; and ep_m and c_m are long-term monthly averages. a_i (i = 1, …, 6) are the model parameters. The superscript plus means $x^+ = \max(x,0)$.

3.4 Model Calibration and Validation

Model calibration and validation are necessary and critical steps in any model application. For most lumped hydrological models, calibration is an iterative procedure of parameter evaluation and refinement, as a result of comparing simulated and observed values of interest. Model validation is an extension of the calibration process. Its purpose is to assure that the calibrated model properly assesses all the variables and conditions which can affect model results. It also demonstrate the ability to predict field observations for periods separate from

the calibration effort and evaluated through qualitative and quantitative measures involving both graphical comparisons and statistical tests (Donigian, 2005).

Conceptual hydrological models are designed to approximate the dominant physical processes of the hydrological cycle with the help of a series of connected mathematical equations (Beven, 2001). The parameters of WASMOD and HBV models cannot be directly determined from field observation or estimated from catchment characteristics, instead determined through the calibration procedure. For HBV model, Monte Carlo procedure was used to investigate the best parameter values using the results of a large number of model runs with randomly generated parameter sets. Using the best parameter set, the first one year period used as a warm up period to initialize the model before actual calibration and the remaining periods were divided in such a way that two-third of the data was used for the calibration and one-third of the data was used for validation. In the case of WASMOD, an automatical optimization is used. After the specification procedure, two-third of the data was used for calibration and the remaining one-third of the data for validation.

It is a common practice to make use of some statistical criteria to evaluate model performance. Among the many model performance indicators, the Nash–Sutcliffe model efficiency coefficient (E) has been widely used to quantitatively describe the accuracy of model output. The coefficient can range from minus infinity to one with higher value indicating better performance (Nash and Sutcliffe,(1970).It is defined as:

$$E = 1 - \frac{\sum (Q_{obs} - Q_{sim})^2}{\sum (Q_{obs} - \overline{Q_{obs}})^2}$$

Where Q_{obs} and Q_{sim} represent observed and simulated discharge respectively and $\overline{Q_{obs}}$ is observer mean value. The value of E represents the extent to which the simulated value is the better predictor of the observed mean. However, the mean value cannot fully indicate how well individual simulated values match observed values. To overcome this limitation, Root mean square error (RMSE) and Relative volume error (RVE) were also employed.

The root mean square error (RMSE) is the measure of differences between values predicted by a model and values actually observed. The root mean square error (RMSE) is defined as;

$$RMSE = \sqrt{\frac{\sum_{t=1}^{n} (Q_{obs_t} - Q_{sim_t})^2}{n}}$$

Where Q_{obs} and Q_{sim} represent observed and simulated discharge respectively and n is a number of observations. RMSE measures the average magnitude of error. Since the errors are squared before they are averaged, it gives relatively high weight to large errors. The value of RMSE can ranges from 0 to ∞ and lower values are better.

Relative volume of error (RVE) tells us how close the simulated value is to the observed value. It gives an indication of how good the simulated value is relative to the size of observed values and defined as;

$$RVE(\%) = \frac{\sum (Q_{obs} - Q_{sim})}{\sum (Q_{obs})} \times 100$$

Where, Q_{obs} and Q_{sim} represent observed and simulated discharge respectively.

4. Results and Discussion

4.1 Evaluation of model performance in reproducing historical records

Statistical and visual comparisons of observed and simulated values were conducted to evaluate the performance of WASMOD and HBV models on different basin scale at different climate zones. In order to compare the statistical performance of the two models, the daily time step result of HBV model is aggregated into monthly values. The evaluated performance statistics for the calibration and validation period are presented in Table 3. For visual comparisons, observed and simulated runoff graphs are presented in the appendix; only the statistical evaluations are briefly discussed here.

The value of Nash–Sutcliffe coefficient (E) in Table 3 indicates that both models are performed quite well in all catchments and it ranges from 0.88 to 0.96 for calibration period and from 0.80 to 0.95 for validation period. The value of E obtained using WASMOD model ranges from 0.88 to 0.94 for calibration and from 0.80 to 0.90 for validation and the highest and the lowest value obtained was at Shuntian and Dembi catchments for calibration period, respectively. The value of E obtained using HBV model ranges from 0.88 to 0.96 for calibration and from 0.84 to 0.95 for validation and the highest and the lowest value obtained was at Shuntian and Dembi catchments for calibration period, respectively. Although E values are in the acceptable range for all basins for both models, relatively slightly higher RMSE and RVE were obtained at Dembi but it is within the acceptable range.

For the validation period, the performance of both models were somewhat reduced in the Hummelvoll catchments. Although there was limited reduction in E, the corresponding low error (RMSE and RVE) obtained increased the confidence of the models performance to

simulate the historical records at acceptable accuracy. Overall, the result shows that both models perform well to reproduce historical records from the three climate zones.

Comparisons of mean monthly runoff values simulated by WASMOD and HBV models with the observed values are as depicted in Fig 4. There is a good agreement in the mean monthly observed runoff with both model simulations. Relatively to other catchments, observed runoff for the months May and July at Dongjiang basin showed a slight difference with mean monthly runoff simulation by both models. The mean monthly runoff simulations of both models were over estimated for the month of August at Elverum and Hummelvoll catchments. WASMOD simulated runoff was also overestimated for September at Hummelvoll catchment. Generally, our result demonstrates that both models were able to reproduce the dynamics of monthly runoff hydrograph for all catchments.

In order to evaluate the capability of WASMOD and HBV models in simulating runoff, the daily result of HBV model is aggregated into monthly values and the monthly model simulated runoff are correlated with the corresponding observed runoff values using linear regression equation $Y = aX + b$ for each catchment. In the regression equation, Y represented model calculated runoff, X is observed runoff, a is slope and b is intercept.

Observed and simulated runoff values were relatively less correlated for Hummelvoll catchment (R^2=0.86) and highly correlated for Shuntian catchment (R^2=.92) using WASMOD model (Fig 5). At the same time using HBV model, observed and simulated runoff were relatively less correlated for Dembi catchment (R^2 = 0.87) and highly correlated for Shuntian (R^2 =0.96) (Fig 6).

Table 3. Model performance statistics obtained using WASMOD and HBV models for different basins and sub-basins during the specified calibration and validation period

Country	Basins and sub-basins	Area (Km^2)	Model	Calibration				Validation			
				Period	E	RMSE	RVE (%)	Period	E	RMSE	RVE (%)
China	Dongjiang	25555	HBV	1978-1983	0.91	15.87	1.64	1984-1988	0.84	15.44	8.98
			WASMOD	1978-1983	0.91	15.57	-1.09	1984-1988	0.83	16.24	4.04
	Shuntian	1357	HBV	1978-1983	0.96	16.37	0.95	1984-1988	0.95	15.53	-4.42
			WASMOD	1978-1983	0.94	21.6	-2.24	1984-1988	0.90	2.23	-8.59
Ethiopia	Didessa	9981	HBV	1987-1992	0.89	11.59	-0.38	1993-1996	0.87	11.18	-11.36
			WASMOD	1987-1993	0.89	11.6	-1.2	1993-1996	0.90	11.14	-5.32
	Dembi	1806	HBV	1987-1993	0.88	27.55	2.38	1994-1998	0.85	25.19	-16.22
			WASMOD	1987-1993	0.88	30.00	-3.85	1994-1998	0.87	24.5	-0.88
Norway	Elverum	15449	HBV	1985-1992	0.90	10.8	0.40	1993-1997	0.90	11.40	-15.5
			WASMOD	1985-1992	0.92	11.49	2.65	1993-1997	0.85	16.21	-1.28
	Hummelvoll	2411	HBV	1980-1988	0.90	12.58	0.90	1989-1995	0.90	12.2	-0.80
			WASMOD	1980-1988	0.89	14.93	-1.87	1989-1995	0.80	17.45	-8.40

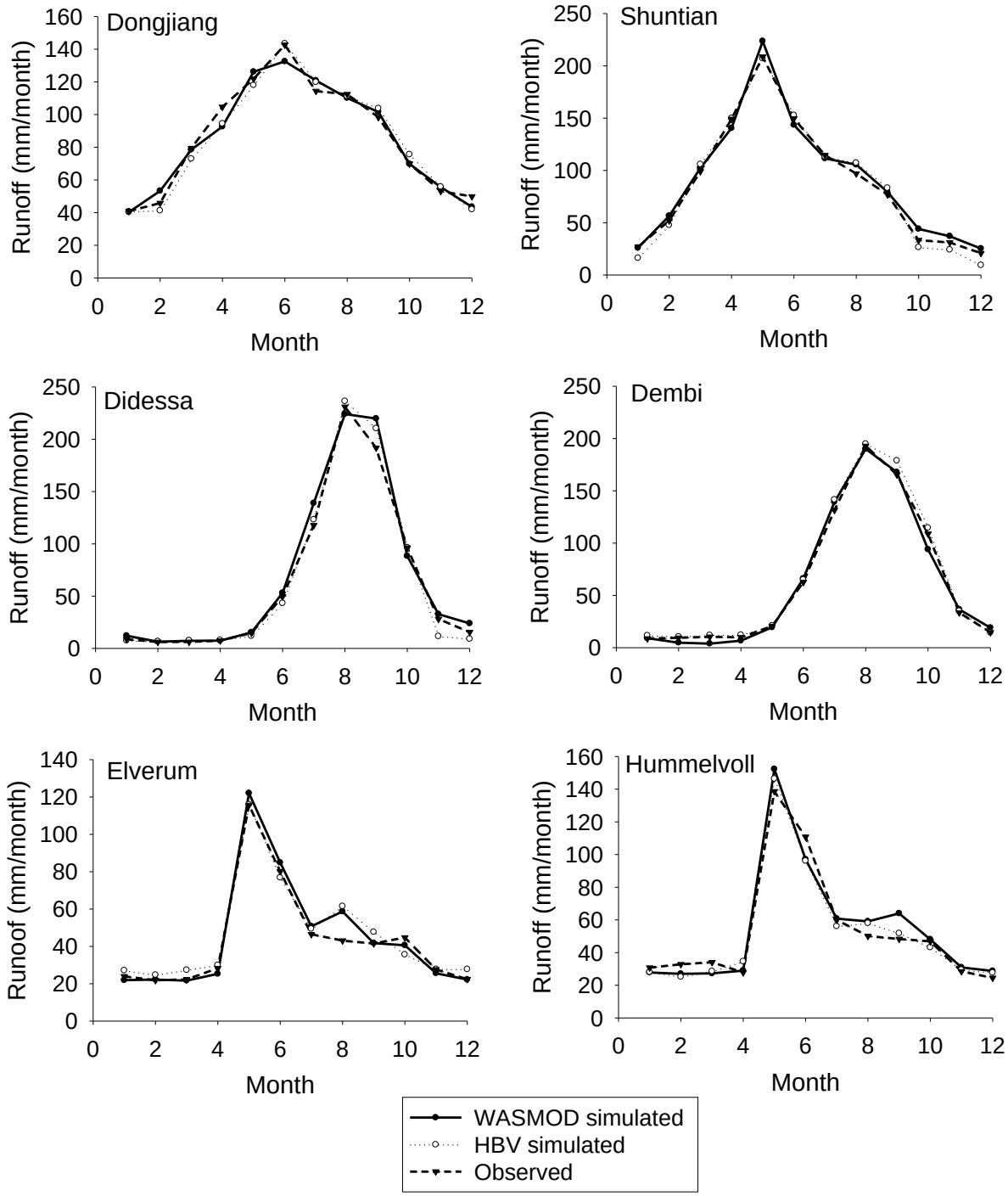

Figure 4. Comparisons of mean monthly observed runoff with WASMOD and HBV simulated runoff in each catchment.

The R^2 values of both models calculation for all catchments indicate that the observed and calculated runoff is well correlated. Concerned the value of the slope, the slope close to one

is relatively less bias and observed at Shuntian, Elverum and Hummelvoll for HBV model and at Shuntian and Didessa for WASMOD model. On the other hand, relatively high bias of slope is observed at Hummelvoll and Dongjiang catchments using HBV and WASMOD models respectively.. The bias in the interception is relatively high at Dongjiang catchment using WASMOD model and at Dembi catchment using HBV model.

Generally, the statistical results and visual observation of observed and calculated runoff graph shows that both WASMOD and HBV models can reproduce historical monthly runoff series at all tested climate zone catchments with an acceptable accuracy. No significant difference exists between the two models in reproducing the historical records. The main purpose of comparing the observed runoff with model simulated value is to check the capability of the models in reproducing the historical records at acceptable accuracy on different climate zones in order to make sure that the simulations under climate change conditions will be predicted well.

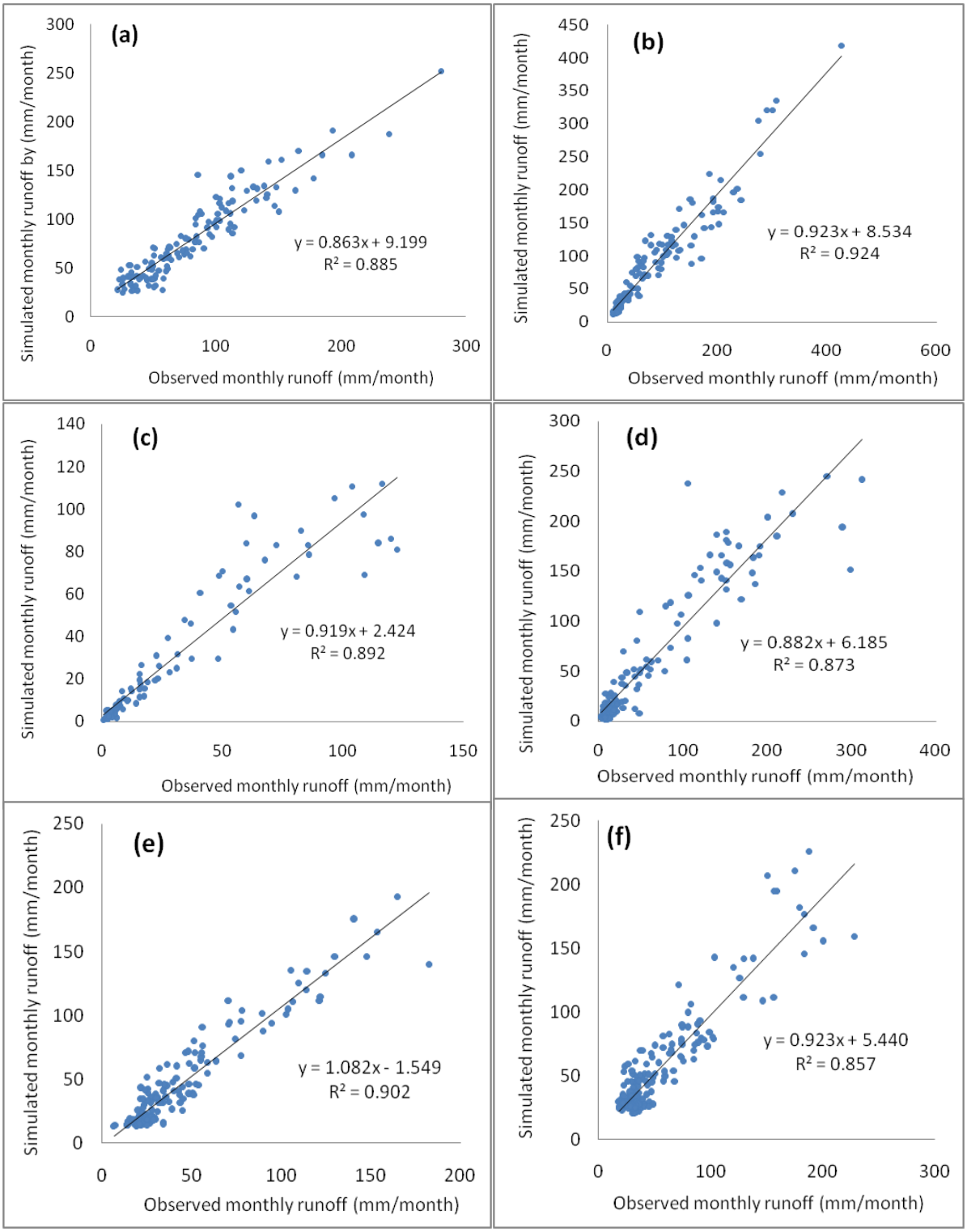

Figure 5. Scattered plot and regression equation of observed versus WASMOD calculated monthly runoff values at (a) Dongjiang, (b) Shuntian, (c) Didessa, (d) Dembi, (e) Elverum, (f) Hummelvoll.

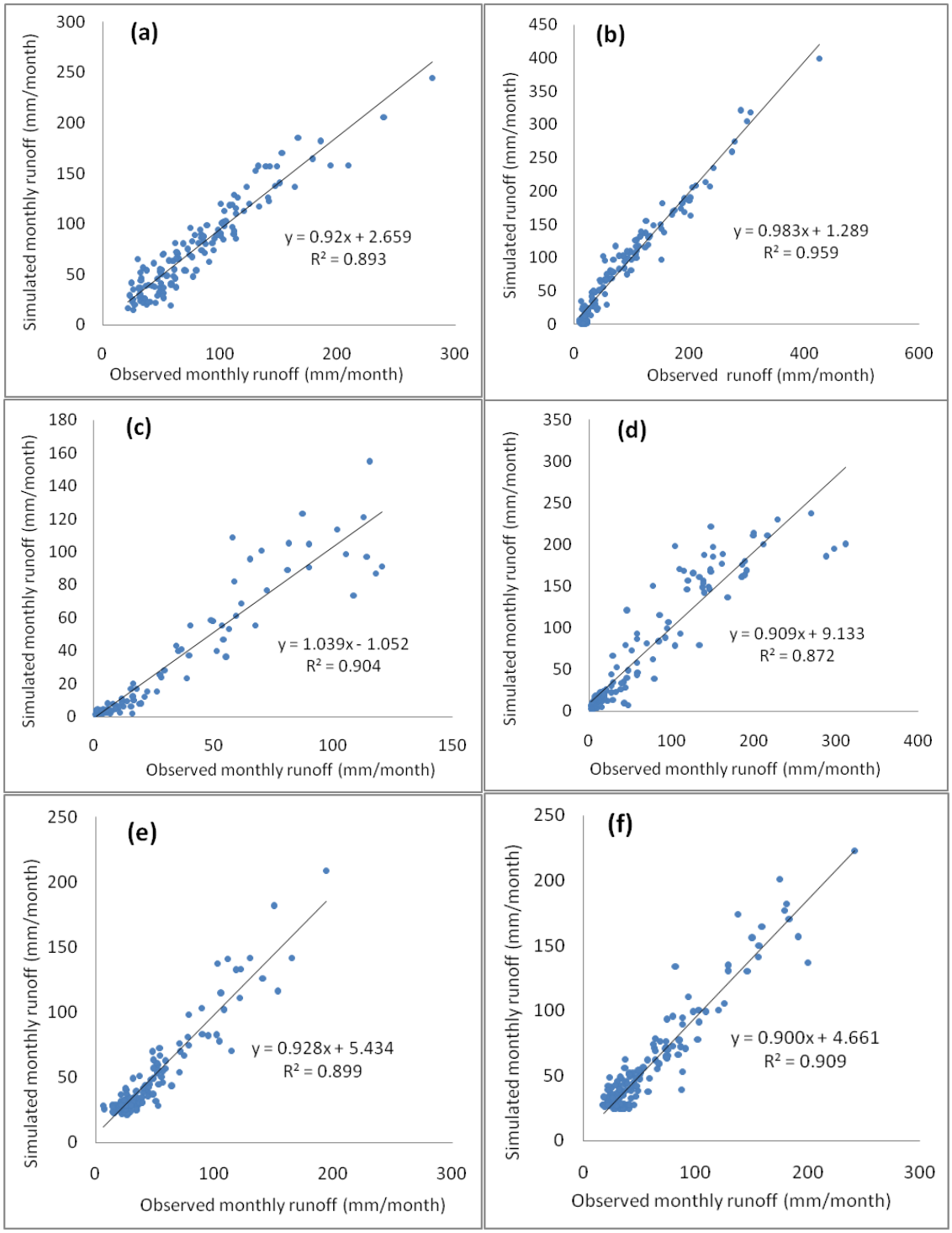

Figure 6. Scattered plot and regression equation of observed versus HBV calculated monthly runoff values at (a) Dongjiang, (b) Shuntian, (c) Didessa, (d) Dembi, (e) Elverum, (f) Hummelvoll.

4.2 Hydrological response of basins for climate change scenarios using WASMOD and HBV models

The ultimate objective of the whole processes is to generate an estimate of change in hydro-climatic variables for a given scenario in different climate zones that characterize the future climate. It is important to be aware of the various environmental responses for climate change and specifically, it is vital for water resource management to be sentient of the effect of climate change on hydro-climatic variables. Obviously, runoff is crucial to provide an indication for the degree of impact of climate change on water resource. The hydro-climatic variables other than runoff included in this study are actual evapotranspiration and soil moisture storage. For all the variables, the change is analyzed on mean annual and monthly average values.

4.2.1 Mean annual runoff change

The outputs from the two hydrological models are analyzed to detect the percentage change in mean annual runoff and the results are presented in Figure 7.

From HBV model result, the potential decrease in mean annual runoff for scenario 6 (ΔP = -20%, and $\Delta T = 4^{o}C$) is relatively bigger from other scenarios for all catchments in the prediction of both models. According to HBV model result using scenario 6, big mean annual runoff change is observed in Didessa catchment and the mean annual run off reduces by 54.2 %. Relatively less change is observed in Hummelvoll catchment and the mean annual runoff reduces by 31.3 %. The change in Dongjiang and Shuntian catchments is -38.7 % and -36.2 % respectively. Based on WASMOD results using the same scenario, the biggest change in annual runoff is also in Didessa catchment and it is estimated 51.7 %

runoff reduction and relatively less change is observed in Hummelvoll catchment and the mean annual runoff reduces by 7.8 %. In addition, the reduction of runoff in Elverum and Dongjiang catchment using the same scenario is by 50.8 % and 51.7 % respectively.

On the other hand, the potential increase in mean annual runoff is observed on scenario – 5 (ΔP = +20%, and $\Delta T = 2^oC$) for all catchments as compare with scenario 6 (ΔP = -20%, and $\Delta T = 4^oC$). According to HBV result, the highest and lowest change is in Didessa and Hummelvoll catchments and the runoff increases by 34.7 % and 10.1 % respectively. In Dongjiang and Elverum catchments, the mean annual runoff increases by 20.6 % and 14.5 % respectively. According to WASMOD results, the highest runoff change is estimated in Didessa and runoff increases by 39.9 %. The lowest change is in Elverum and it is estimated 15.1 % runoff increase. In Dongjiang basin, the runoff increases by 28.4 %.

For scenario 3 (ΔP = 0%, and $\Delta T = 2^oC$), in the absence of precipitation change, According to WASMOD result, mean annual runoff reduces by 14.2 %, 9.1 % and 0 % in Elverum, Didessa and Dongjiang catchments. Based on HBV result, the mean annual runoff reduces by 10.2 %, 12.7 %, and 7.6 % in Elverum, Didessa, and Dongjiang catchment respectively. Beside to this, when we compare for scenario 8 (ΔP = 0%, and $\Delta T = 4^oC$), if temperature further increases by 4^oC, the mean annual reduction estimated by WASMOD is 26.1 %, 16.8 %, and 0 % in Elverum, Didessa and Dongjiang whereas according to HBV estimation, the runoff reduces by 13.9 %, 22.6 % and 20.7 % in Elverum, Didessa and Dongjiang catchments.

The relative change in mean annual runoff due to temperature change (from 2^oC to 4^oC) for a given precipitation (from -20 % to 20 %) is quite different for different region. According to HBV result, the runoff reduction ranges from 8.4 % to 12.3 % for Elverum catchment,

from 7.9 % to 11.6 % for Didessa catchment and from 4.9 to 7.6 % for Dongjiang catchment. According to WASMOD result, the mean annual runoff reduction ranges from 9.7 % to 13.6 % for Elverum catchment, from 5.0 % to 11.1 % for Didessa catchment, and for Dongjiang catchment, there is no change.

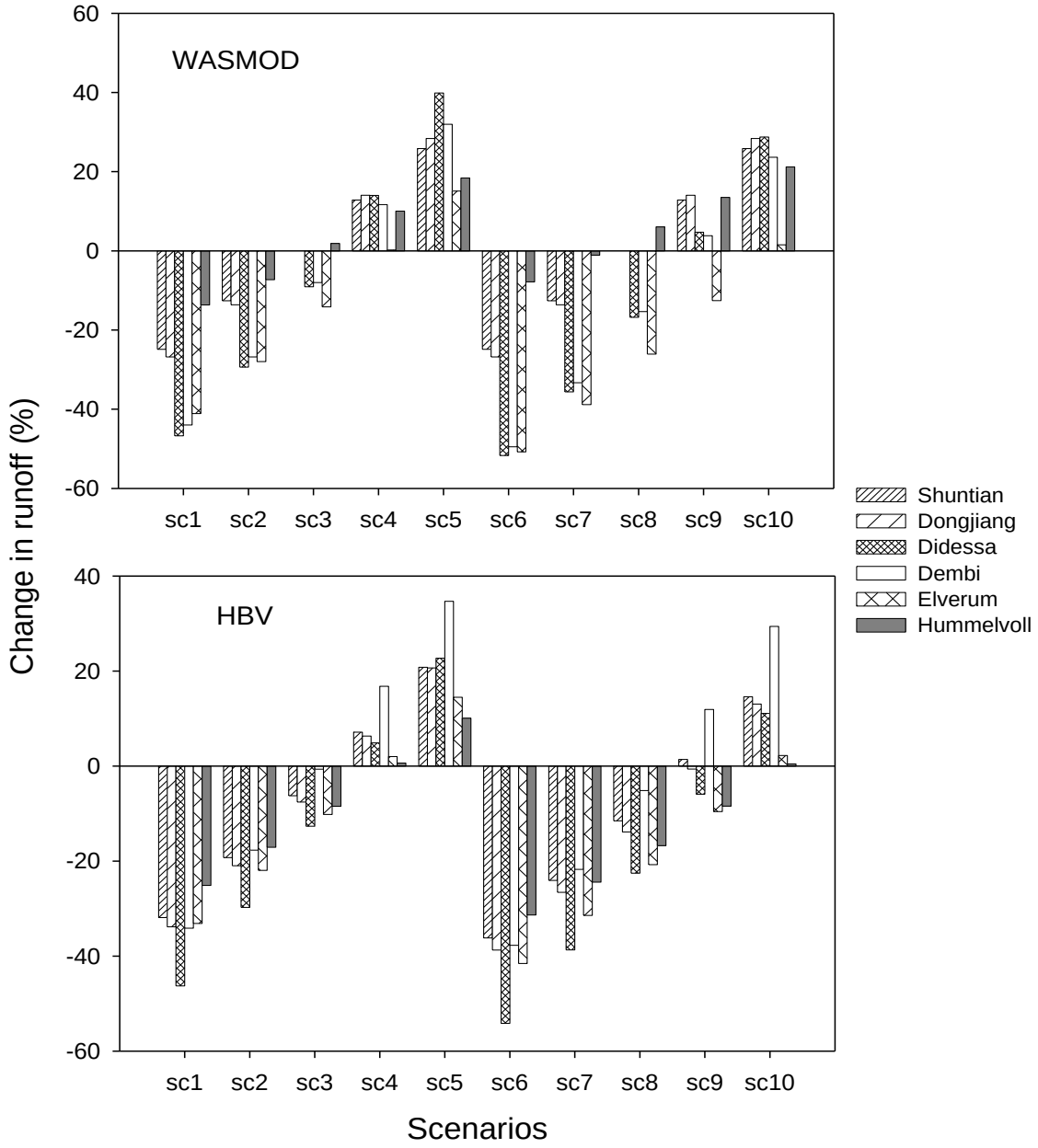

Figure 7. Mean annual runoff change estimated by HBV model (upper graph) and WASMOD model (lower graph) using 10 scenarios in different catchments

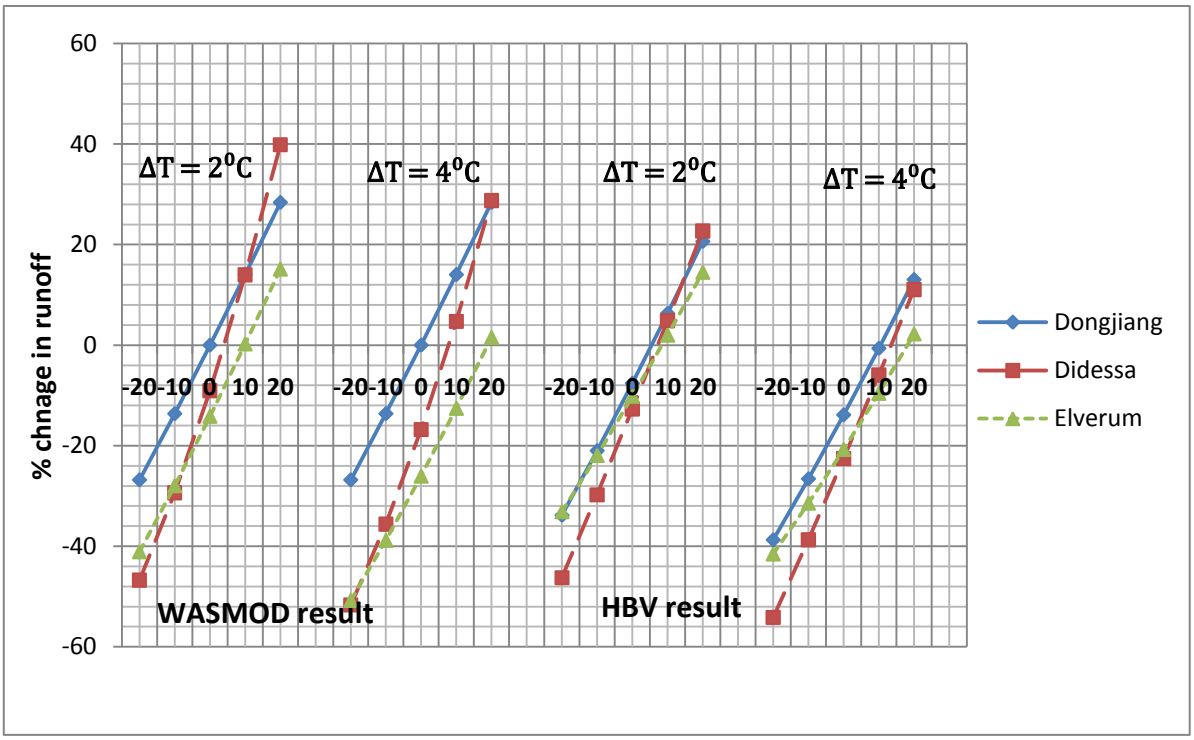

Figure 8. Mean annual runoff change estimated by WASMOD and HBV models

The significant change in mean annual runoff on the three basins for all climate change scenarios are shown in Fig 8. Different climatic zones may response differently for the same scenario and hydrological models. In WASMOD prediction as it is shown in Figure 8, Didessa basin response sensitively for each change in precipitation for both 2 ^{o}C & 4 ^{o}C temperature change. While the response of Dongjiang and Elverum basins are almost similar and not as sensitive as Didessa basin. In all catchment cases, the temperature change from 2^{o}C to 4^{o}C for a given precipitation change increases the magnitude of changes in mean annual runoff. The prediction of WASMOD and HBV model as it is shown in Fig 8, Didessa basin is sensitive for each precipitation change and the magnitude of mean annual runoff change is high in the case of WASMOD as compare with HBV result. Dongjiang and Elverum basins are not sensitive as Didessa basin.

4.2.2 Mean annual actual evapotranspiration change

Models results for ten future climate change scenarios on six catchments are illustrated in Fig 9. As it is shown in the figure, the mean annual actual evapotranspiration change detected by HBV model for all catchments are relatively higher as compare with WASMOD model results. According to HBV result, actual evapotranspiration change for Elverum catchment is as high as 55.5 % when temperature change by 4^{o}C and where as the change detected by WASMOD for the same catchment and for the same scenario is 49.2 %. The mean annual actual evapotranspiration change detected using both models for Elverum catchment shows that the catchment is more sensitive for change in temperature than for change in precipitation and it reflects that the limiting factor for actual evaporation is energy than moisture.

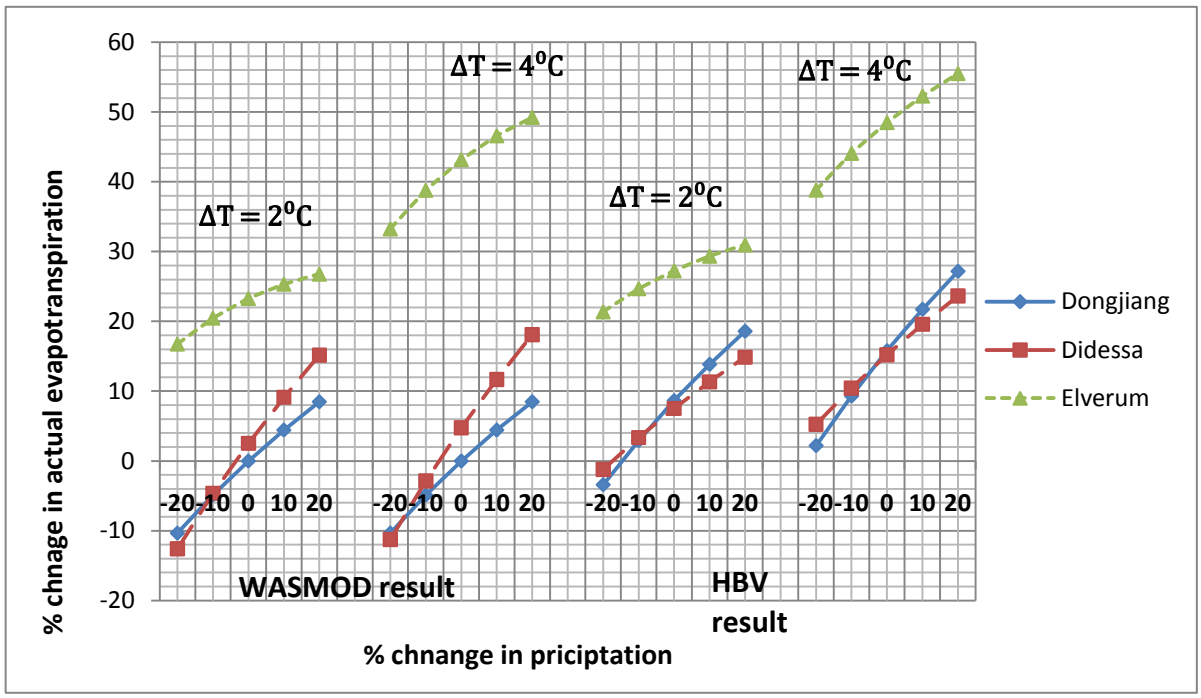

Figure 9. Mean annual actual evapotranspiration change estimated by WASMOD and HBV models

As WASMOD result shows that the mean annual actual evapotranspiration change of Dongjiang catchment is relatively less sensitivity for both temperature and precipitation change as compare with HBV result.

According to WASMOD result, the mean annual actual evapotranspiration of Didessa catchment is more sensitive for precipitation change than temperature change but according to HBV result, the catchment is relatively less sensitive for precipitation change and moderately sensitive for temperature change.

4.2.3 Mean annual soil moisture storage change

The percentage change in mean annual soil moisture storage in response to ten climate change scenarios using WASMOD and HBV models are shown in Fig 10.

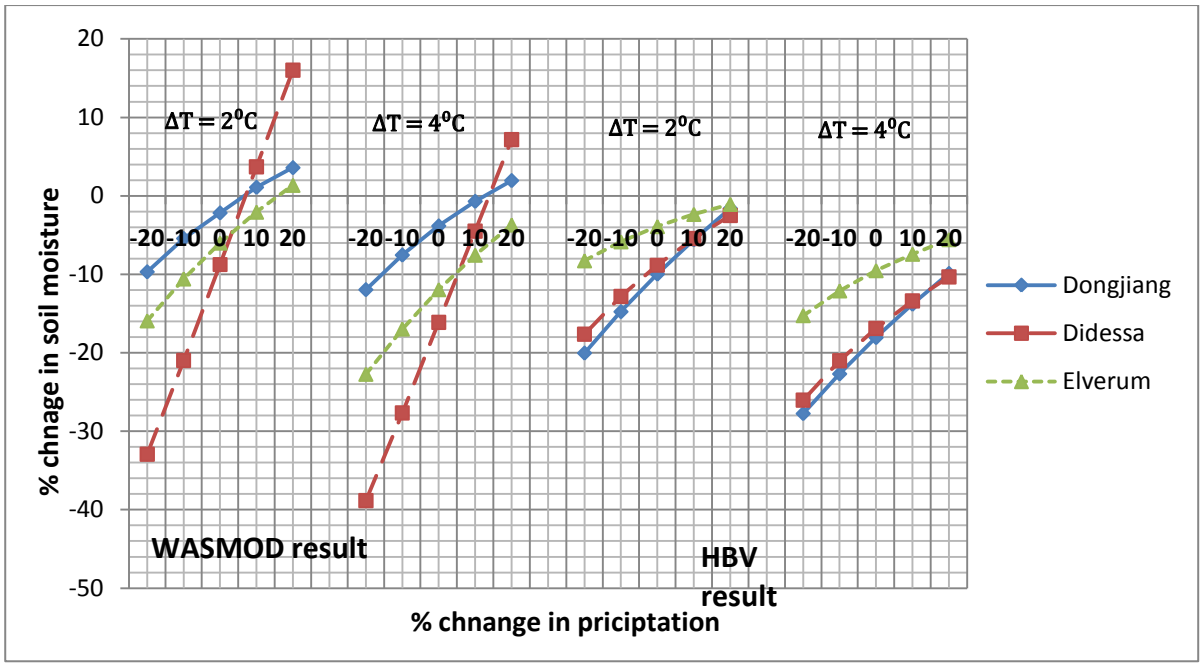

Figure 10. Mean annual soil moisture storage change estimated by WASMOD and HBV models for each catchment

From WASMOD results, the mean annual change of soil moisture in Didessa catchment is relatively sensitive for a given precipitation change than the other catchments but according to HBV result, the catchment is not uniquely sensitive for precipitation change. In the case of Elverum catchment, the mean annual soil moisture change is more sensitive for precipitation change using WASMOD as compare with HBV results. The sensitivity of Dongjiang catchment for precipitation change is almost similar for both WASMOD and HBV model prediction but the sensitivity of the catchment for temperature change is in the case of HBV is more sensitive than WASMOD results.

From HBV a result, the change in soil moisture storage is relatively negative for all scenarios on all catchments and this result reflect that the temperature increase scenario is significantly reduces the soil moisture storage in all regions. The differences in soil moisture storage change estimate by WASMOD in different catchments is high due to the fact that the model does not have upper and lower threshold limit for soil moisture storage where as in the case of HBV model, the lower and upper soil moisture storage limit is defined during parameter optimization procedure.

4.2.4 Mean monthly runoff change

The application of scenario 1 ($\Delta T = 2^{o}C$ & $\Delta P = -20$ %) and the percent of change in mean monthly runoff estimated by the two models in the three climate zone catchments are illustrated in the Fig 11. The Fig shows that in the case of Elverum catchment, the percentage change in mean monthly runoff rises in April and considerably drops from May to throughout the year in both model predictions. Except April, the estimated mean monthly runoff change is negative. The pattern of mean monthly runoff change detected by the two models is relatively similar but the magnitude is significantly different.

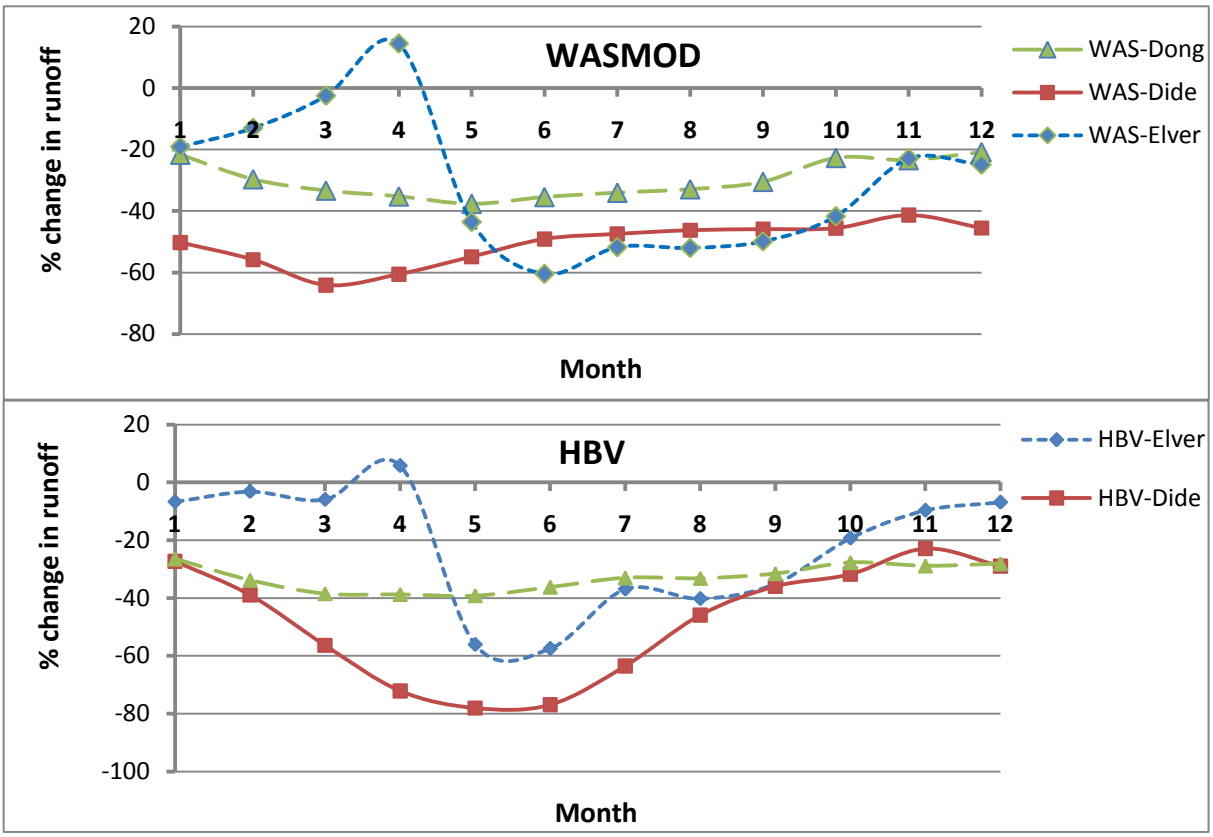

Figure 11. Comparison of mean monthly change in runoff simulated by WASMOD (upper graph) and HBV (lower graph) for scenario 1 ($\Delta T = 2^{o}C$ & $\Delta P = -20$ %)

The application of scenario 1 for Didessa catchment results that there is significant difference between HBV and WASMOD model calculated changes in mean monthly runoff. According to WASMOD result, runoff reduced by 64.1 % in March and it is the maximum reduction but in November, the runoff reduced by 41.3 % and it is the lowest reduction. When we see the estimation of HBV model, the maximum reduction of mean monthly runoff is attended in May and it is 78.0 % and relatively lowest reduction of runoff is in November and it is by 22.9 %.

In the case of Dongjiang catchment, the application of scenario 1 results that the percentage changes detected by both models are almost similar and the highest change is in May and the lowest change in January in both model prediction. The highest percentage change in mean

monthly runoff is -39.2 % and -37.6 % and the lowest is-26.5 % and -21.6% by using HBV and WASMOD models respectively.

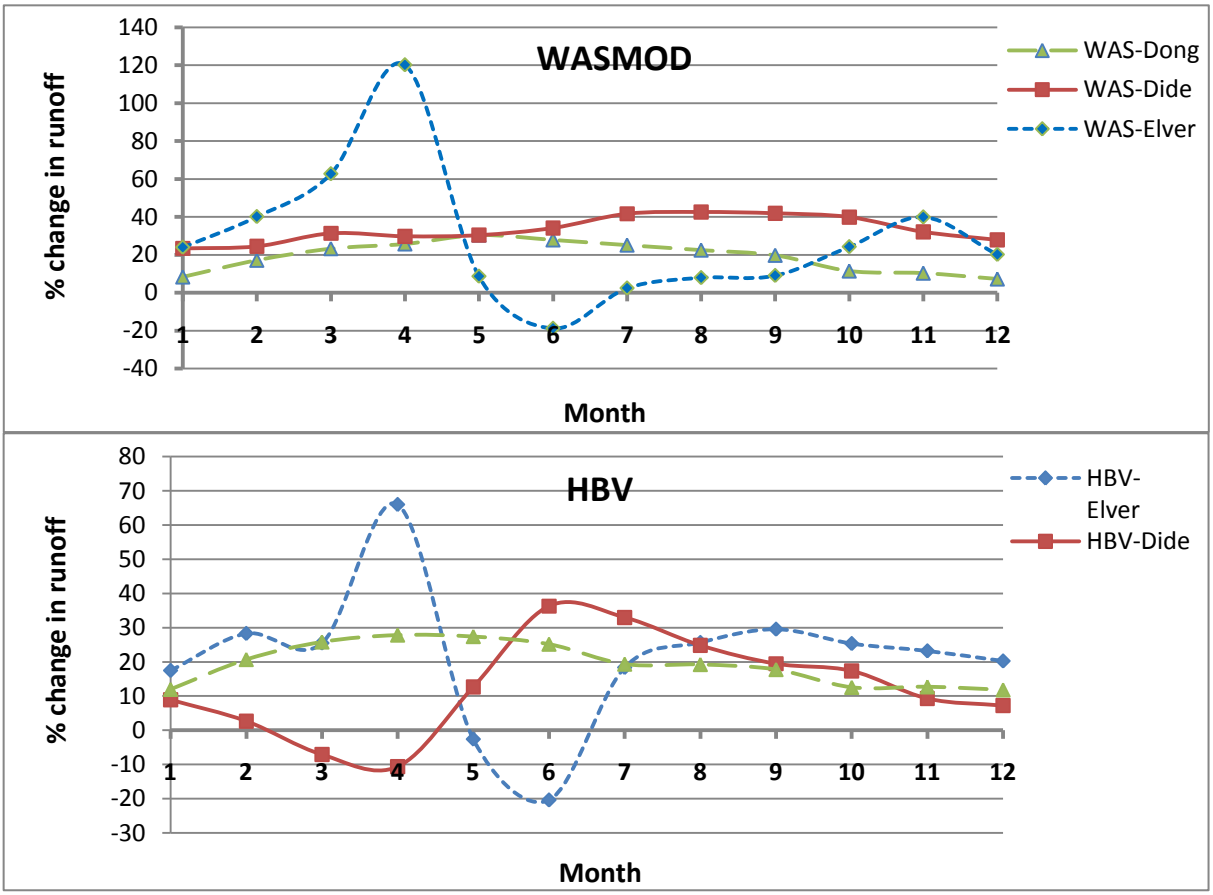

Figure 12. Comparison of mean monthly change in runoff simulated by WASMOD (upper graph) and HBV (lower graph) for scenario 5 ($\Delta T = 2^{o}C$ & $\Delta P = +20$ %)

The application of scenario 5 ($\Delta T = 2^{o}C$ & $\Delta P = +20$ %) and the percent change in mean monthly runoff predicted by the two models for the three catchments are illustrated in Fig 12. According to WASMOD result as it is shown in the figure, the mean monthly runoff calculation for Elverum catchment is rises as high as 120.1 % in April and considerably drops to -18.8 % in June and the change is positive for the rest of months. On the other hand, the prediction of HBV model for the same catchment shows the same trend except the difference in magnitude of changes which is the highest in April and lowest in June and it is 66.0 % and -20.4 % respectively.

According to WASMOD calculation for Didessa catchment, the percentage change in mean monthly runoff ranges from 42.5 % in August to 23.4 % in January. Whereas according to HBV prediction, the runoff reduced by 10.6 % in April and increases by 36.3 % in June.

In Dongjiang catchment, the trend of percent change in mean annual runoff predicted by using the two model is almost similar and it ranges from 7.2 % to 30.4 % in December and May in the case of WASMOD prediction and 11.8 % to 27.9 % in December and April in the case of HBV prediction.

By the application of scenario 6 ($\Delta T = 4^{o}C$ & $\Delta P = -20$ %), the percent change in mean monthly runoff predicted by both WASMOD and HBV model is shown in Fig 13. As it revealed in the figure, According to WASMOD result for Elverum catchment, the percent change in mean monthly runoff is positive in March and April and the change is highest in April (42 %) but for the rest of the months, the percent change is negative and the lowest change attends in Jun and it is -47 %. Based on HBV model prediction, the percent of change in mean monthly runoff ranges from 0.3 % in April to -76.8 % in May.

According to WASMOD estimation of change in mean monthly runoff for Didessa catchment, it ranges from -73.8 % in March to -46.6 % in November. Whereas in line with HBV prediction, the percent change in mean monthly runoff ranges from -10.6 % in Jun to 36.3 % in April.

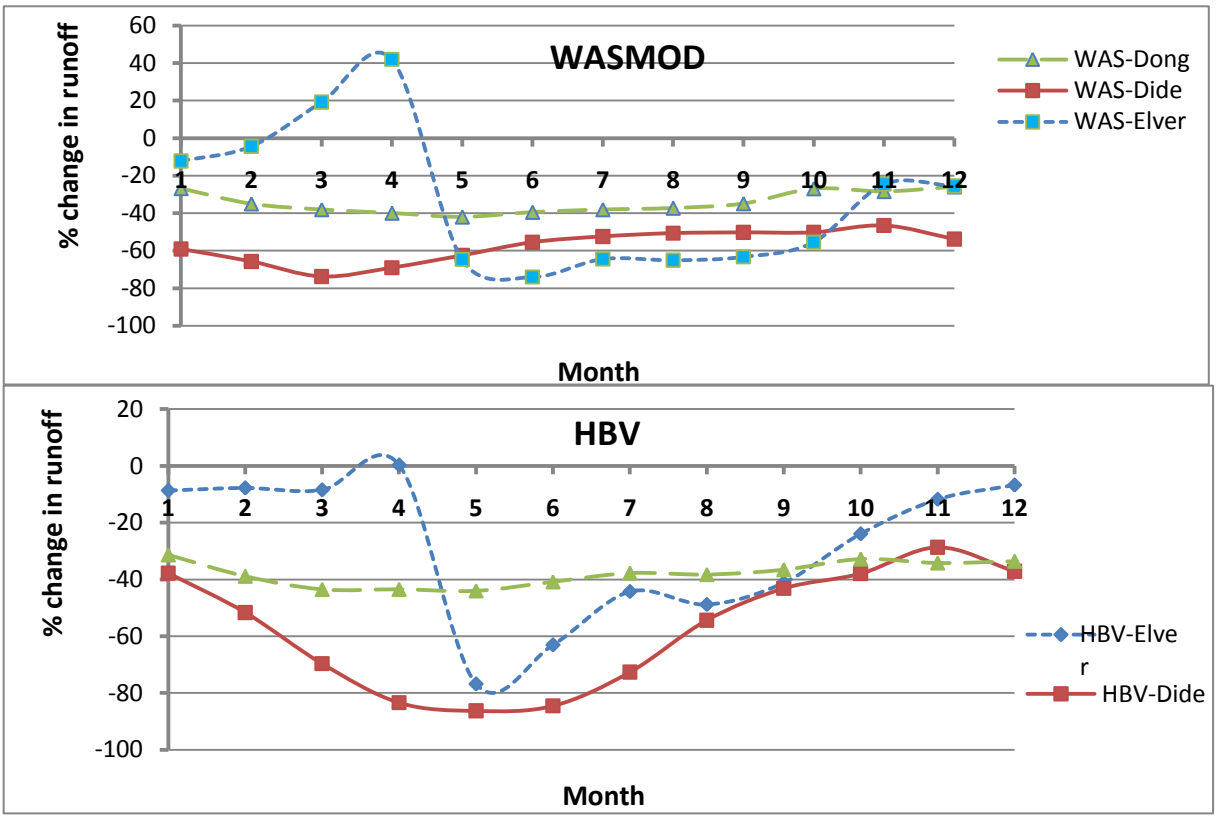

Figure 13. Comparison of mean monthly change in runoff simulated by WASMOD (upper graph) and HBV (lower graph) for scenario 6 ($\Delta T = 4^{o}C$ & $\Delta P = -20$ %)

For Dongjiang catchment, the percent change in mean monthly runoff is not considerably fluctuating in both model cases and the range is from -42.0 % in May to -26.0 % in December in line with WASMOD prediction and from -44.0 % in May to -31.3 % in January according to HBV prediction.

By the application of scenario 10 ($\Delta T = 4^{o}C$ & $\Delta P = +20$ %), the percent change in mean monthly runoff for the three catchments using WASMOD and HBV models are shown in Fig 14. As it is shown in the figure, according to WASMOD estimation for Elverum catchment, the percent change in mean monthly runoff ranges from 4.8 % to 187.4 % in October to April. The negative change (reduction in mean monthly runoff) occurred from Jun to September and the percent change ranges from -14.1 % to -45.1 %. Whereas in the

case of HBV prediction, the percent change ranges from 70.5 % to 7.3 % from July to April and during May and June, the percent change is -56.8 % and -35.0 % respectively.

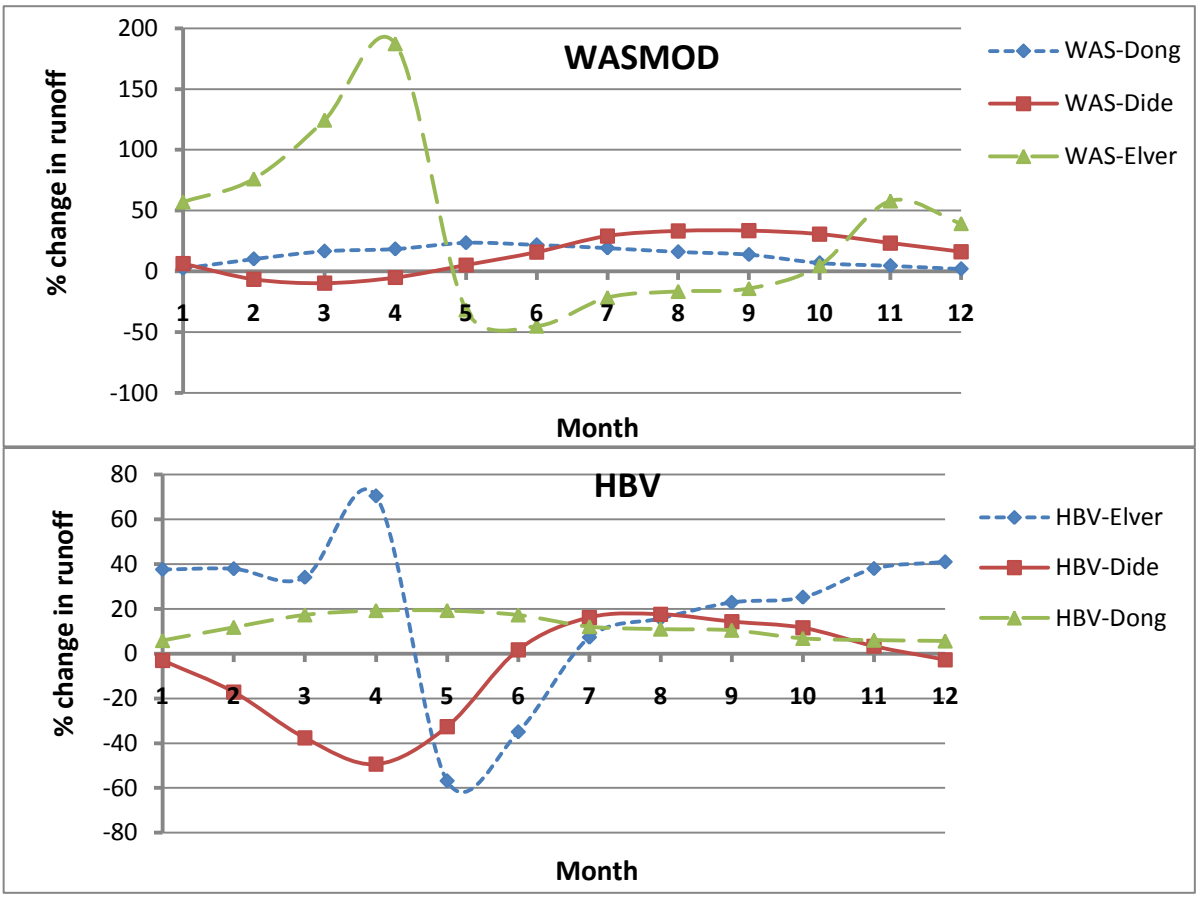

Figure 14. Comparison of mean monthly change in runoff simulated by WASMOD (upper graph) and HBV (lower graph) for scenario 10 ($\Delta T = 4^{o}C$ & $\Delta P = +20$ %)

According to the estimation of WASMOD for Didessa catchment, the percent change in mean monthly runoff is negative from February to April and it becomes positive from May to January. The maximum positive change attended in September and it is 33.4 %. The lowest change is occurred in March and it is -9.6 %. In line with HBV model prediction, from December to May, the percent change ranges from -32.6 % to -2.8 % and the maximum reduction of runoff is in April. On the other hand, from June to November the percent change ranges from 1.7 % to 17.5 % and maximum increase occurs in August.

In line with WASMOD prediction of mean monthly runoff change for Dongjiang catchment, the change ranges from 2.0 % in December to 23.5 % in May. According to HBV model prediction, the percent change in mean monthly runoff is not fluctuated as in the case of WASMOD and the change ranges from 5.6 % in December to 19.3 % in May.

4.2.5 Mean monthly Actual evapotranspiration change

The application of scenario 1 ($\Delta T = 2^{o}C$ & ΔP = -20 %) and the percent change in mean monthly actual evapotranspiration predicted by the two models for the three catchments are illustrated in Fig 15. As it is shown from the figure, the percent change in actual evapotranspiration predicted by WASMOD for Elverum catchment ranges from 0 % to 25.7 % and the change is highest in April. For Didessa catchment, the change ranges from -46.9 % in February to 0.1 % in June. For Dongjiang catchment, the change ranges from -4.8 % in May to -1 % in January.

On the other hand, the prediction of HBV model for the same scenario shows that the percentage change in actual evapotranspiration for Elverum catchment ranges from -8.9 % in November to 61.5 % in October. Mean annual evapotranspiration reduced only on November otherwise it increases for the other months. For Didessa catchment, the percentage change ranges from -46.9 % in February to 10.1 % in November and Mean monthly actual evapotranspiration reduces from December to May and increases from June to November. The prediction for Dongjiang catchment shows that, the percent change ranges from -10.6 % in December to 0.1 % in June and except June, in other months the actual evaporation decreases.

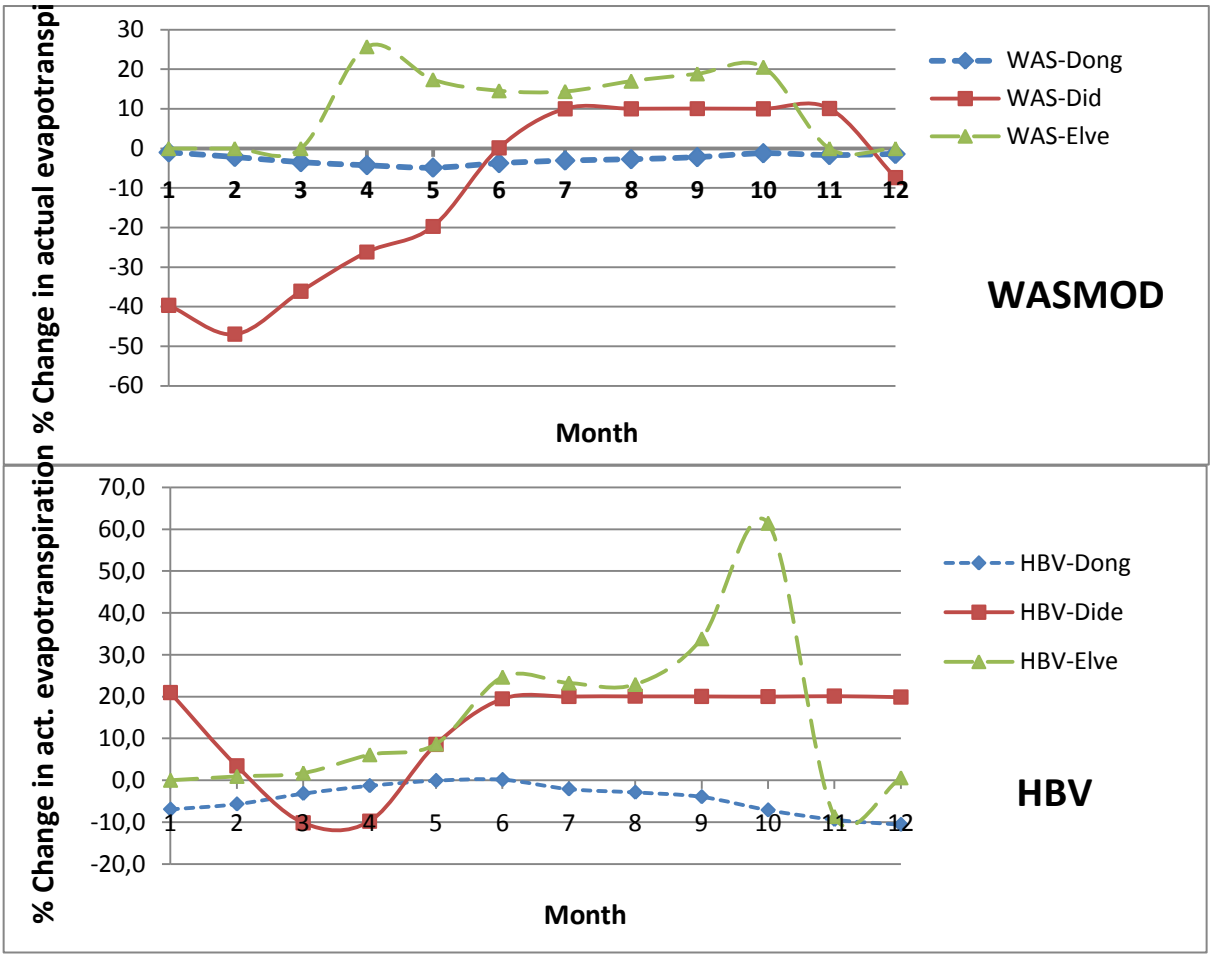

Figure 15. Comparison of mean monthly change in actual evapotranspiration simulated by WASMOD (upper graph) and HBV (lower graph) for scenario 1 ($\Delta T = 2^{o}C$ & $\Delta P = -20$ %)

The application of scenario 5 ($\Delta T = 2^{o}C$ & $\Delta P = +20$ %) and the percent change in mean monthly actual evapotranspiration predicted by the two models for the three catchments are shown in Fig 16. The prediction of WASMOD shows that the percent change in mean monthly actual evapotranspiration for Elverum catchment reaches its maximum in April and it is 34.6 % and from April to October, the change ranges from 24.9 % to 34.6 %. For Didessa catchment, it ranges from 8.2 % in May to 17.5 % in January. For Dongjiang catchment, the percent change in mean monthly actual evapotranspiration ranges from 12.7 % in January to 20.3 % in May.

Based on the prediction of HBV model, for Elverum catchment, the percent change in mean monthly actual evapotranspiration ranges from -16.8 % in November to 61.9 % in October. For Didessa catchment, the percent change ranges from 12.6 % in March to 22.3 % in January. For Dongjiang catchment, the percent change ranges from 12.3 % in January to 23 % in April.

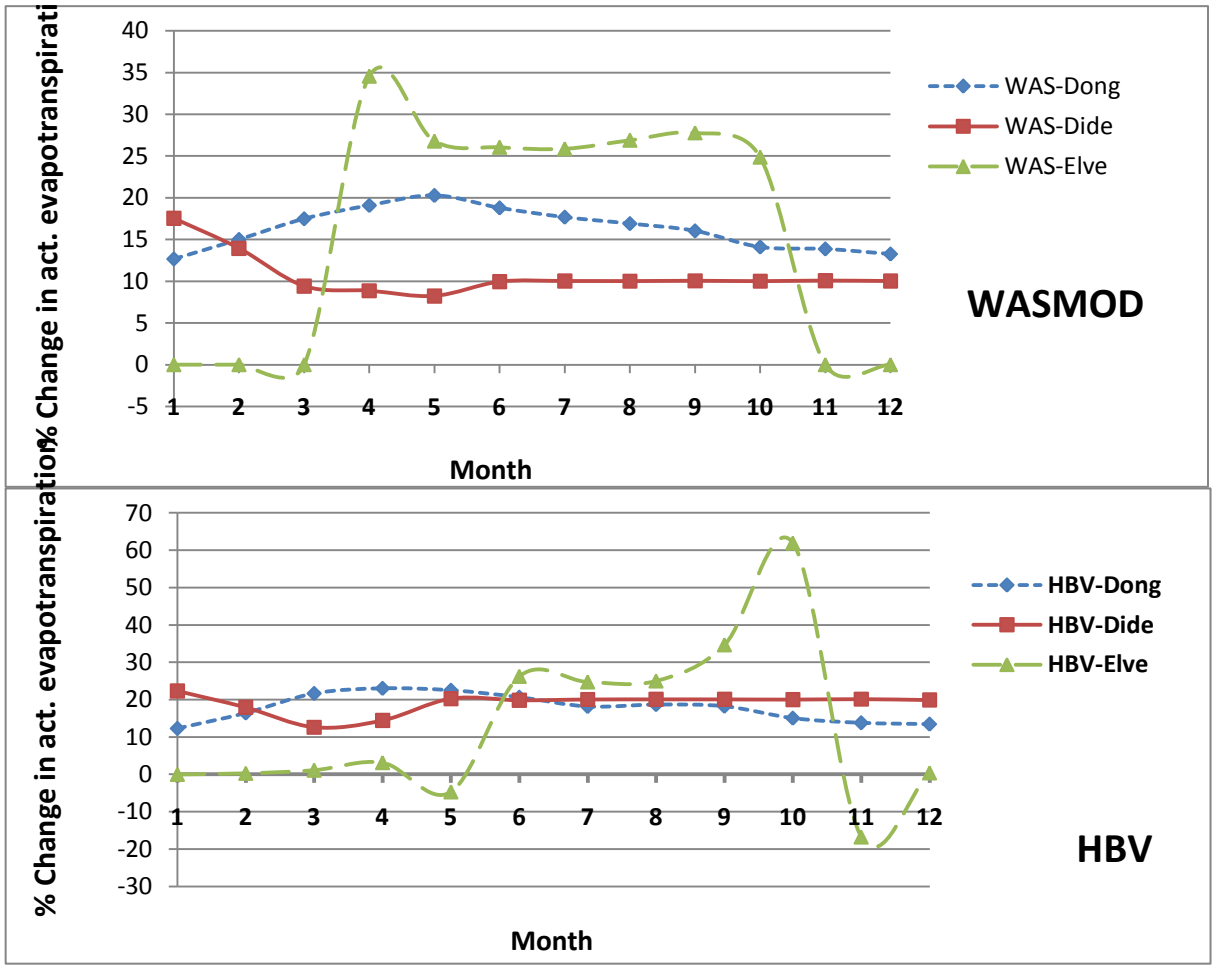

Figure 16. Comparison of mean monthly change in actual evapotranspiration simulated by WASMOD (upper graph) and HBV (lower graph) for scenario 5 ($\Delta T = 2^{o}C$ & $\Delta P = +20$ %)

The application of scenario 6 ($\Delta T = 4^{o}C$ & $\Delta P = -20$ %) and the percent change in mean monthly actual evapotranspiration predicted by the two models for the three catchments are shown in Fig 17. As it is shown in the graph, the percent change in mean monthly actual evapotranspiration predicted by WASMOD for Elverum catchment ranges from 0 % in

March to November to 53.9 % in April. For Didessa catchment, it ranges from -54.2 % in February to 20.1 % in September. Actual evapotranspiration increases from June to November and decreases from December to May. For Dongjiang catchment the percent change in mean monthly actual evapotranspiration ranges from 1.9 % in May to 4.9 % in October.

The prediction of HBV model for Elverum catchment using scenario 6 also shows that, the percent change ranges from 6.1 % in December to 100.7 % in October. For Didessa catchment, the mean monthly actual evapotranspiration change ranges from -21.8 % in March to 40.1 % in September. For Dongjiang catchment, it ranges from -11.1 % in December to 9.1 % in May.

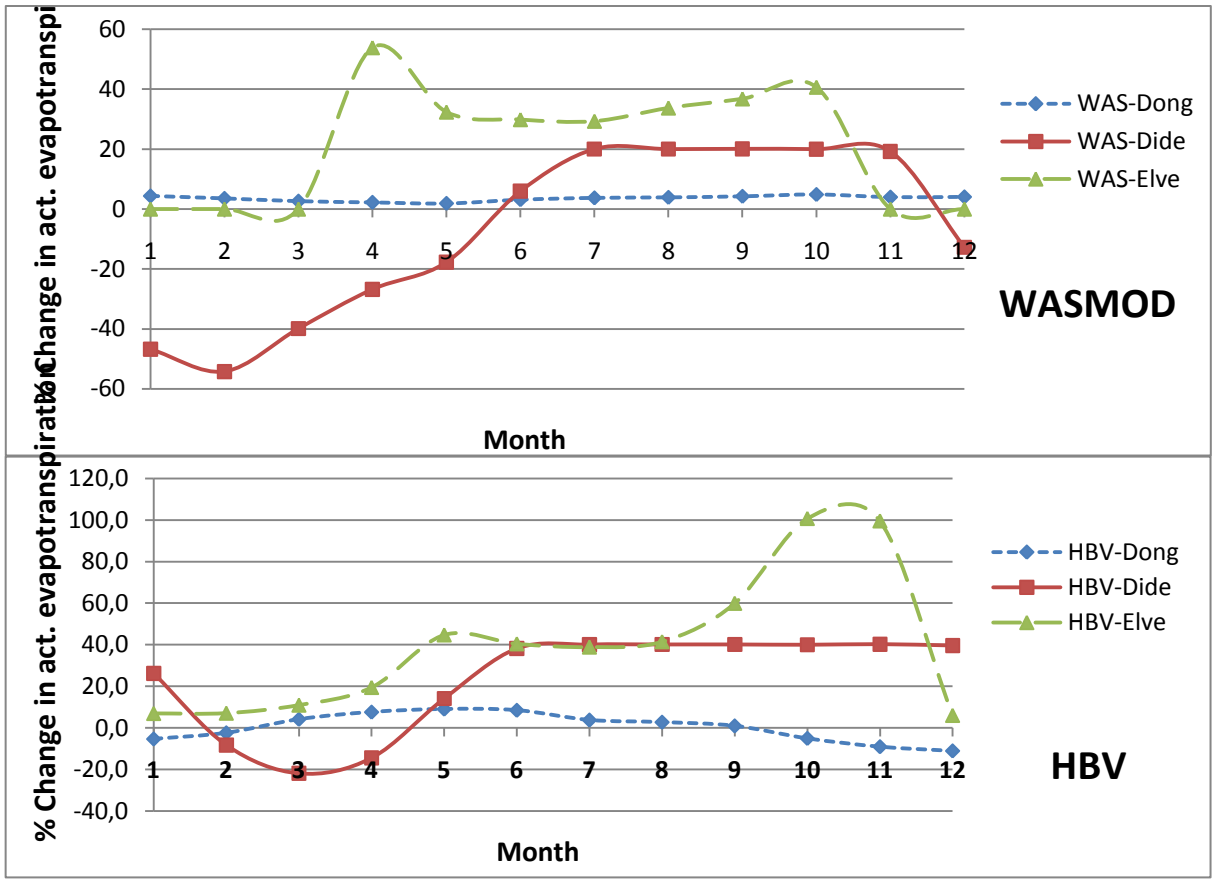

Figure 17. Comparison of mean monthly change in actual evapotranspiration simulated by WASMOD (upper graph) and HBV (lower graph) for scenario 6 ($\Delta T = 4^{o}C$ & $\Delta P = -20$ %)

The application of scenario 10 (ΔT = 4°C & ΔP = +20 %) and the prediction of mean monthly actual evapotranspiration of the two models for the three catchments are revealed in Fig 18. As it is shown in the figure, the percent change in Mean monthly actual evapotranspiration estimated by WASMOD for Elverum catchment ranges from 0 % to 65 %. From November to March, there is no change in actual evapotranspiration whereas in April it increases by 65 % and the fluctuation of change is relatively high as compare with the other catchments. For Didessa catchment, it ranges from 5.6 % in February to 25.2 % in May. For Dongjiang catchment, it ranges from 19.8 % in January to 29.7 % in May.

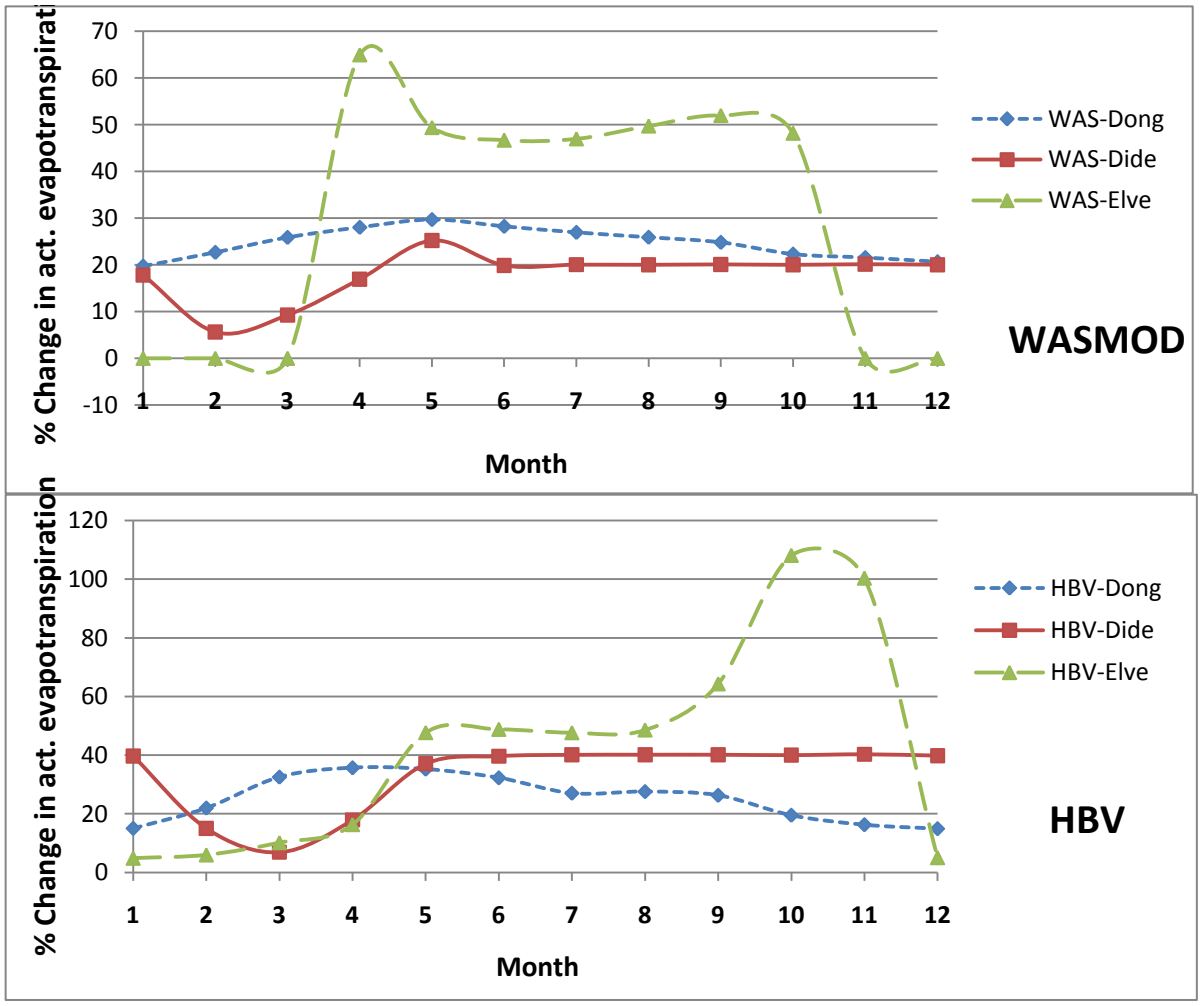

Figure 18. Comparison of mean monthly change in actual evapotranspiration simulated by WASMOD (upper graph) and HBV (lower graph) for scenario 10 (ΔT = 4°C & ΔP = +20 %)

According to HBV model prediction, for Elverum catchment, the percent change in mean monthly actual evapotranspiration ranges from 4.9 % in January to 108.1 % in October. For Didessa catchment, it ranges from 6.9 % in March to 40.1 % July to September. For Dongjiang catchment, it ranges from 14.9 % in December to 35.7 % in April.

4.2.6 Mean monthly soil moisture storage change

Soil moisture change is one of the relevant variables for assessing climate change impact on hydrological regimes of basins since it incorporates the integrated effect of precipitation, evaporation and runoff.

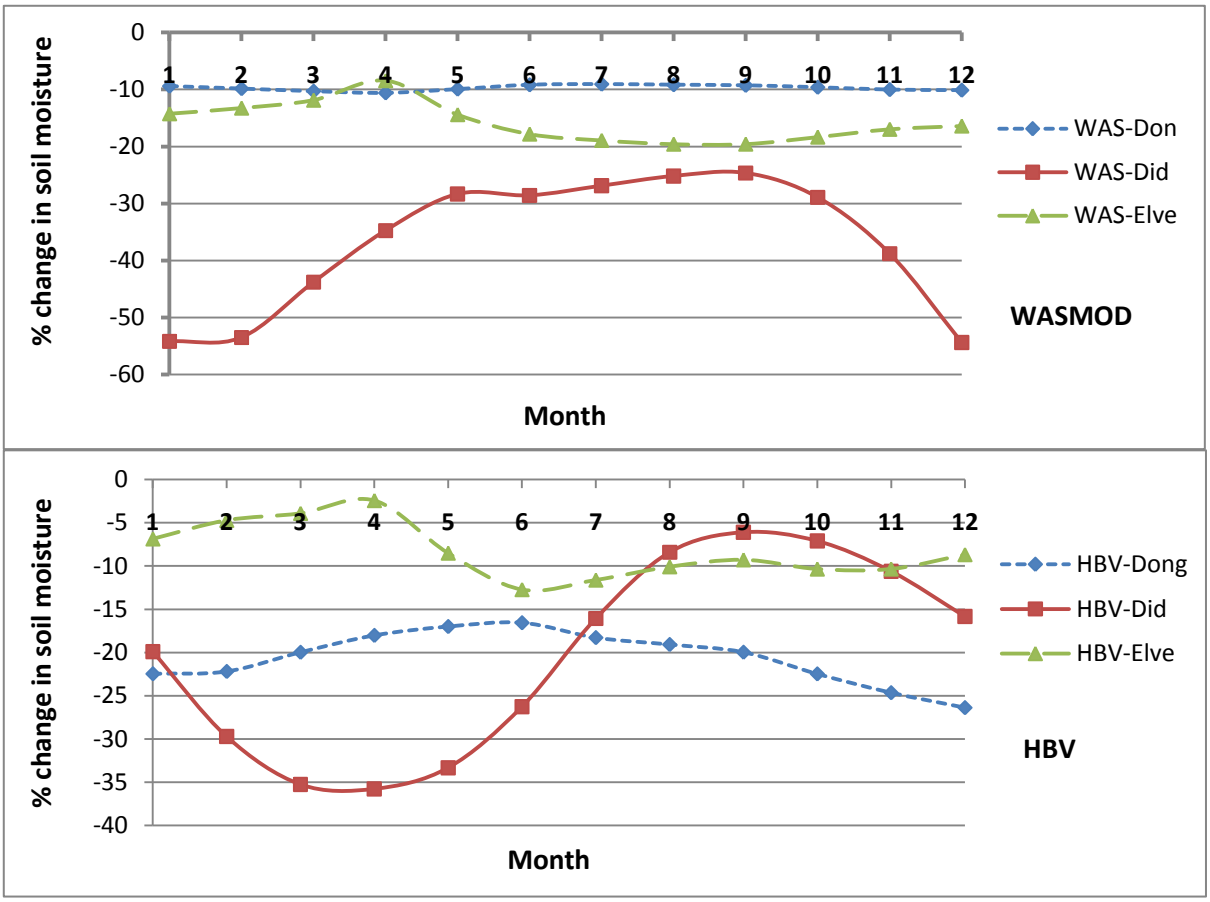

Figure 19. Comparison of mean monthly change in soil moisture storage simulated by WASMOD (upper graph) and HBV (lower graph) for scenario 1 ($\Delta T = 2^{o}C$ & $\Delta P = -20$ %)

As it is shown in Fig 19, mean monthly soil moisture storage decreases in all regions in response to the application of scenario 1 when 2^0C temperature increases combine with 20 % precipitation reduction. However, the seasonal variation of soil moisture change is relatively less in Dongjiang and Elverum basin as compare with Didessa basin in both models estimation.

The percent change in mean monthly soil moisture storage in response to scenario 1 ($\Delta T = +2^0C$ & ΔP = -20 %) using WASMOD model ranges from -9.1 % in July to -10.6 % in April for Dongjiang basin, from -8.4 % in April to –19.6 % in August for Elverum basin, and from -54.4 % in December to -24.7 % in September for Didessa basin.

According to HBV model prediction of mean monthly soil moisture storage change as shown in Fig 19, the estimated change is relatively small in Dongjiang and Elverum basin as compare with Didessa and has a constant seasonal pattern with slightly higher in April for Dongjiang and in June for Elverum basin. The percent change in mean monthly soil moisture storage ranges from -2.4 % to -12.7 % for Elverum, and from -16.6 % to -26.4 % for Dongjiang basin. The estimated change for Didessa basin for the same scenario shows relatively bigger seasonal variation and it ranges from -35.8 % in April to -6.1 % in September.

Fig 20 shows that mean monthly change in soil moisture storage at each basin for scenario 5 ($\Delta T = +2^0C$ & ΔP = + 20 %). The estimation of change in soil moisture storage by using WASMOD model shows that the soil moisture change is relatively large and positive for Didessa basin and it ranges from 6.2 % in April to 20.8 % in December. The change is highest during wet season and lowest during dry season.

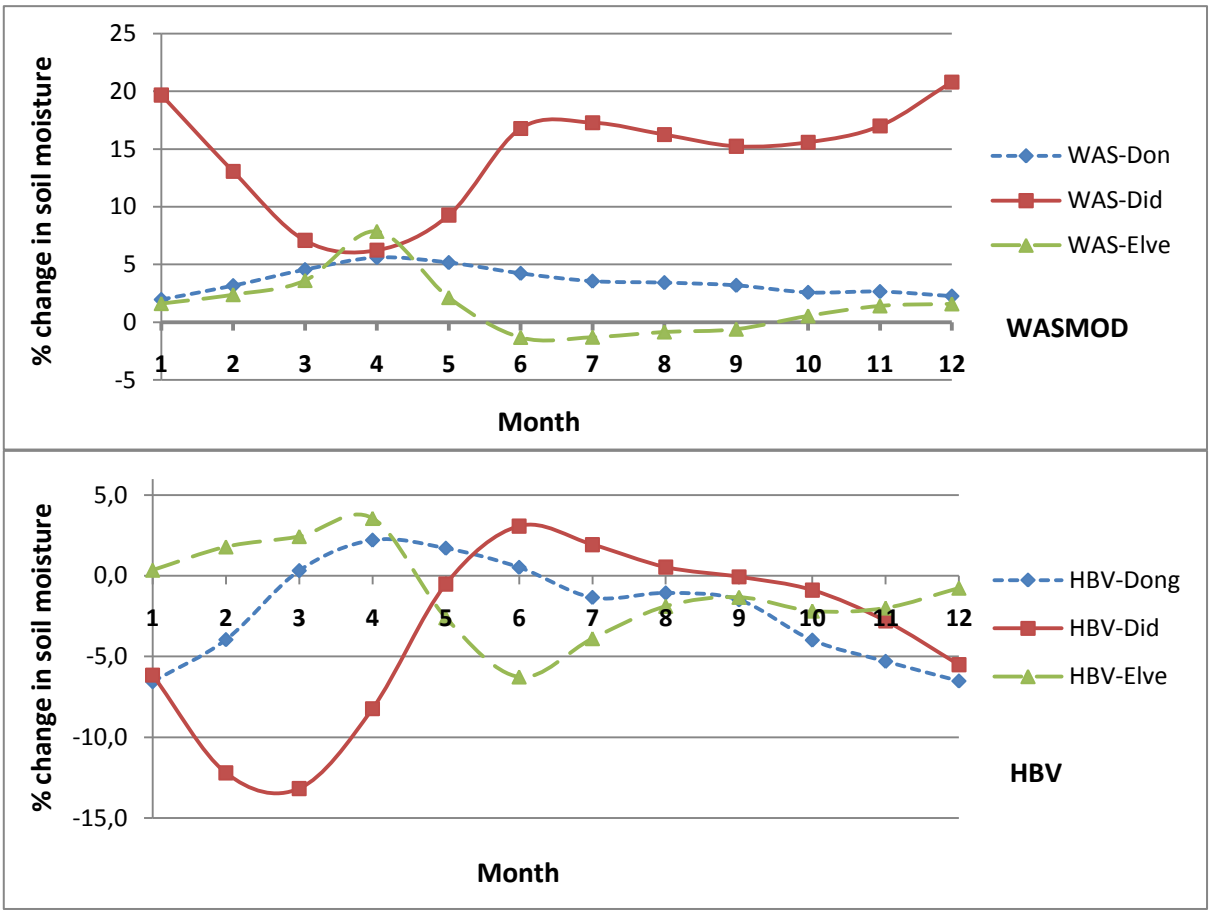

Figure 20. Comparison of mean monthly change in soil moisture storage simulated by WASMOD (upper graph) and HBV (lower graph) for scenario 5 ($\Delta T = 2^{o}C$ & $\Delta P = +20$ %)

For Dongjiang basin, the estimated change is positive and it ranges from 2.0 % to 5.6 % with small seasonal variation. For Elverum basin, the change is relatively small and negative from June to September and positive from October to May. The change ranges from -1.3 % in June to 7.9 % in April.

Based on HBV model estimation of mean monthly moisture storage change, seasonal variation is observed in all basins. For Elverum basin, the percent change ranges from -6.3 % in June to 3.6 % in April and the change are positive from January to April and negative from May to December. For Didessa basin, the change substantially dropped -13.2 % in March. The change is negative from September to May during dry and hot season. On the

other hand, the change rises to 3.1 % in June and the change is positive from June to August. For Dongjiang basin, the change ranges from -6.6 % in January to 2.2 % in April and the change is negative from July to February and positive from March to June.

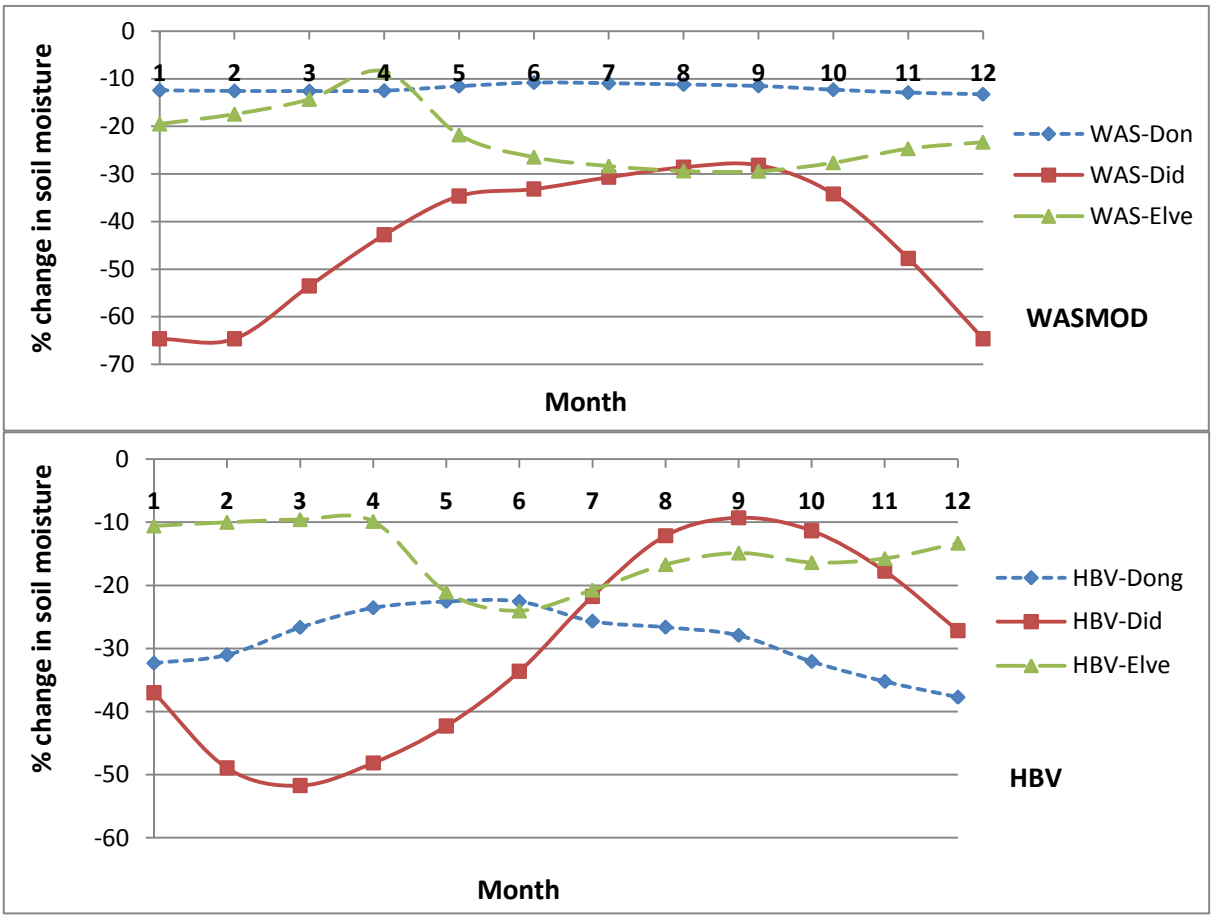

Figure 21. Comparison of mean monthly change in soil moisture storage simulated by WASMOD (upper graph) and HBV (lower graph) for scenario 6 ($\Delta T = 4^{o}C$ & $\Delta P = -20$ %)

The investigation of climate change impact on soil moisture storage by applying scenario 6 ($\Delta T = +4^{0}C$ & $\Delta P = -20$ %) using WASMOD model are illustrated in Fig 2. It shows that for Didessa basin, a distinct decrease in soil moisture up to 64.4 % from December to February during hot and dry period. The change ranges from -64.6 % to -28.1 %. For Dongjiang basin, the seasonal variation is small. The percent change in mean monthly moisture storage is negative throughout the year and it ranges from -10.8 % in January to -13.2 % in December.

For Elverum basin, the soil moisture storage ranges from -29.4 % in August to -8.5 % in April.

According to HBV model result from the application of scenario 6, seasonal variability of soil moisture storage change is high for all catchments and at the same time the percent change is negative. In Didessa basin, the percent change ranges from -51.7 % to -19.6 % in March and September respectively. In Dongjiang basin, it ranges from -37.7 % in December to -22.6 % in May, and in Elverum basin, it ranges from -9.6 % in March to -24 % in June.

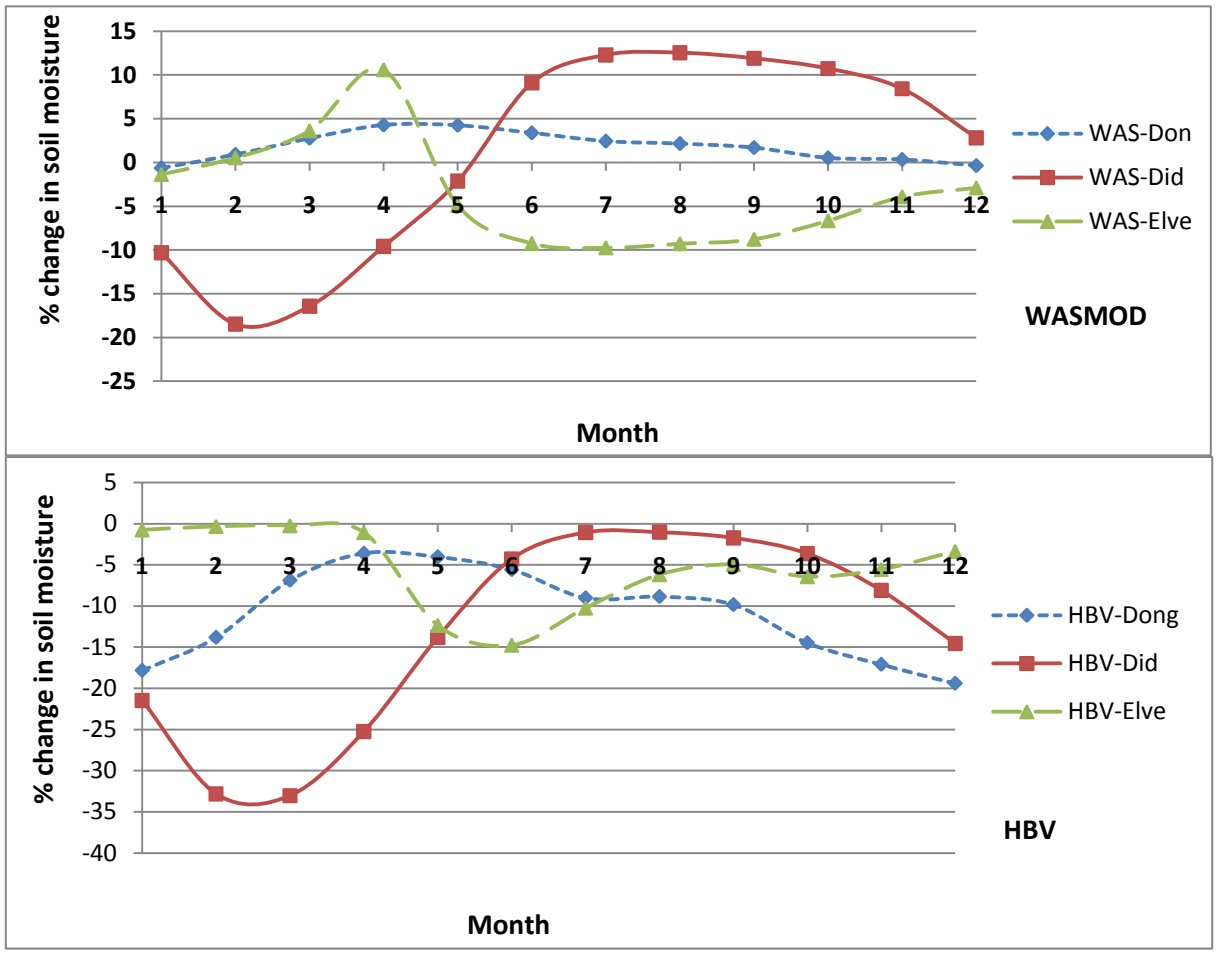

Figure 22. Comparison of mean monthly change in soil moisture storage simulated by WASMOD (upper graph) and HBV (lower graph) for scenario 10 ($\Delta T = 4^{o}C$ & $\Delta P = +20$ %).

Estimate of soil moisture storage change by applying scenario 10 ($\Delta T = +4^0C$ & $\Delta P = +20\%$) using WASMOD and HBV models are shown in Fig 22. The prediction of WASMOD shows that for Didessa basin, the seasonal variability of soil moisture storage change highest and it ranges from -18.5 % in February to 12.5 % in August with negative change from January to May and positive from June to December. For Elverum basin, the seasonal variation is relatively lower as compared with Didessa but higher when it compared with Dongjiang basin and the percent change in soil moisture storage ranges from -9.7 % in July to 10.6 % in April. For Dongjiang basin, the seasonal variability of soil moisture storage is relatively less as compared with the other two basins and it ranges from -0.6 % in January to 4.3 % in April.

The investigation of soil moisture change using scenario 10 by HBV model shows higher variability for all basins and at the same time the percent change is negative. For Didessa basin, the percent change ranges from -28.1 % in February to -1.4 % in July, and For Dongjiang basin; it ranges from -3.6 % in April to -19.4 % in December.

4.3 Sensitivity analysis of the two models in different climatic regions using climate change scenarios

4.3.1 Sensitivity of the two models to estimate mean annual runoff change

Model sensitivity analysis involved the application of 10 scenarios (the combination of two temperature change and 5 precipitation change scenarios). These sensitivity analyses are expressed as change in mean annual runoff by WASMOD and HBV models in different climate zone basins (Fig 23). Both models show that mean annual runoff is more sensitive to change in precipitation than to change in temperature for all basins. In Didessa and Elverum basins, the change in mean annual runoff calculated by WASMOD is more sensitive for

precipitation change than HBV model results whereas in Dongjiang basin, the sensitivity of the two models for precipitation change is almost similar. The magnitude of mean annual runoff change estimated by WASMOD is relatively higher than HBV result In Dongjiang basin while, in Didessa basin, WASMOD estimate is higher for precipitation increase scenario and in Elverum for precipitation reduction scenarios. Therefore, the overall sensitivity of mean annual runoff estimation by WASMOD and HBV models to climate change scenarios across different climate zone basins are different.

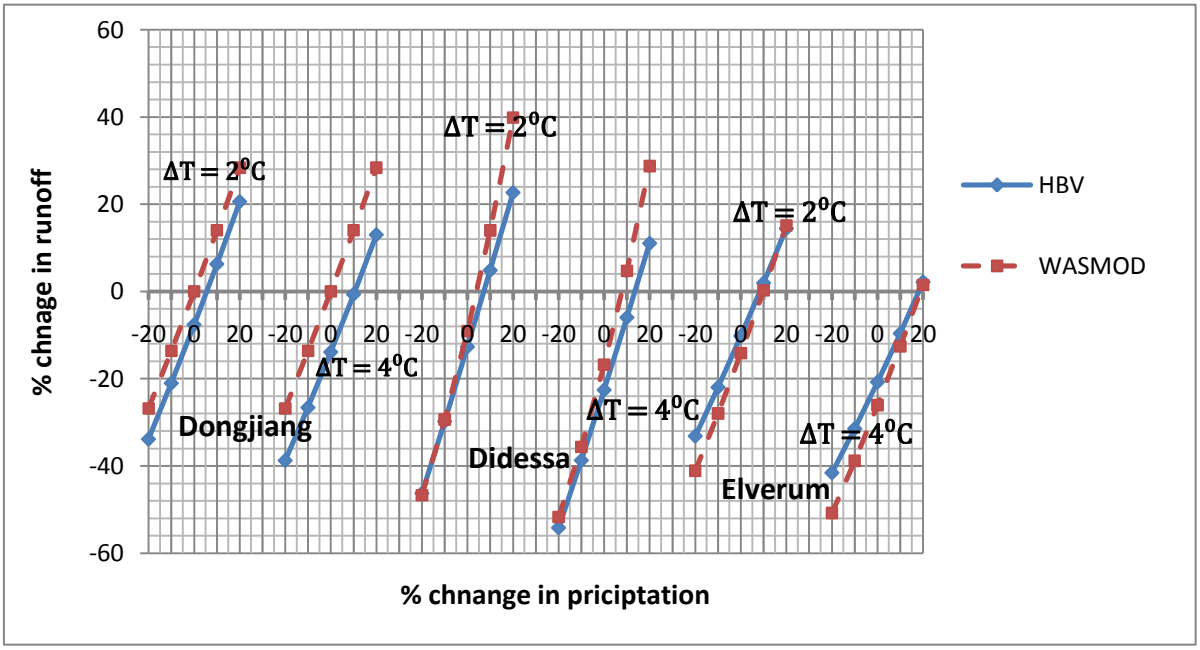

Figure 23. Comparison of mean annual change runoff in response to precipitation increase for a given temperature change using WASMOD and HBV simulation for each basin.

4.3.2 Sensitivity of the two models to estimate mean annual actual evapotranspiration change

Model sensitivity analysis was carried out based on 10 synthetic scenarios. As it is shown in Fig 24, there is significant difference between the magnitudes of change estimated by the two models. HBV model estimates relatively higher change for all basins as compared with WASMOD model. Both models confirm that Elverum basin is more sensitive in actual

evapotranspiration change in response to temperature change but relatively less sensitive for precipitation change. The magnitude of mean annual actual evapotranspiration change estimated by HBV model is higher than WASMOD in all catchments. The mean annual actual evaporation change estimated by WASMOD in Didessa basin is more sensitive for precipitation change than temperature change as compared to HBV model estimate and the sensitivity of HBV model for temperature change is higher as compare with WASMOD model. The sensitivity of both models in terms of estimating mean annual actual evapotranspiration in Dongjiang basin is moderately sensitive for both temperature and precipitation change but there is significantly difference in magnitude for temperature increase by 4 ^{o}C scenario.

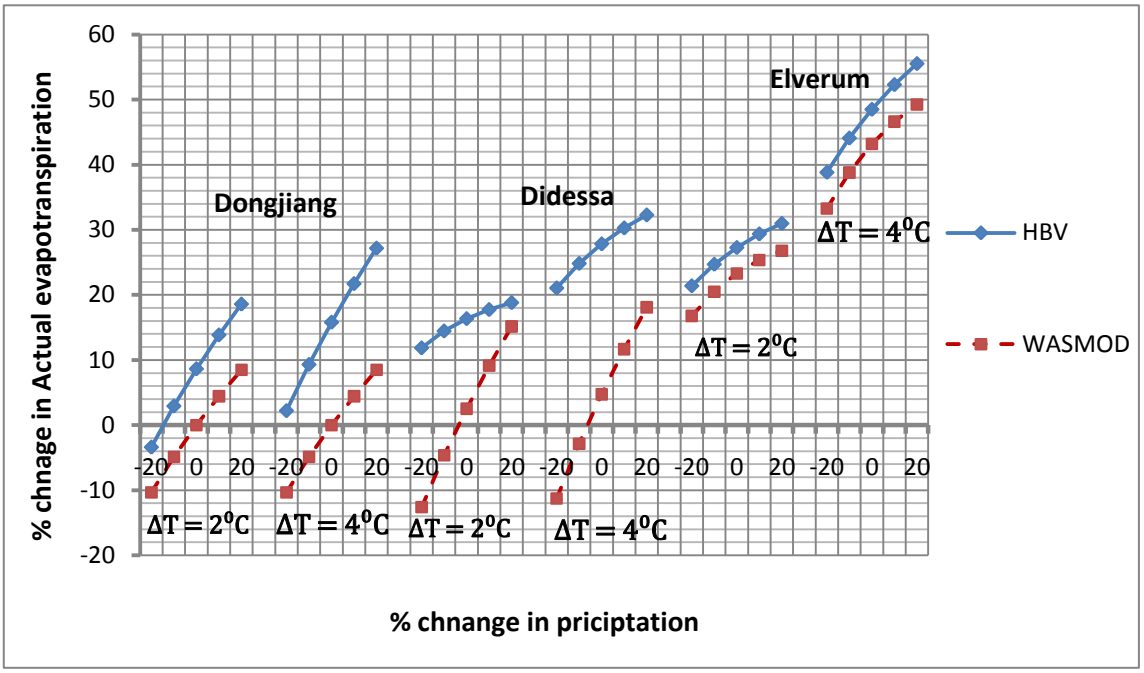

Figure 24 Comparison of mean annual change in actual evapotranspiration in response to precipitation increase for a given temperature change using WASMOD and HBV simulations for each basin.

4.3.3 Sensitivity of the two models to estimate mean annual soil moisture storage change

Sensetivity analysis of WASMOD and HBV models to estimate mean annual soil moisture storage change in each climatic region is illustrated in Fig 25. As it is shown in the figure, the estimations of the two models have relatively similar pattern except the magnitude difference for Dongjiang basin but the magnitude of difference increases when for temprature change scenario increase from 2^0C to 4^0C. in Didessa basin, WASMOD is more sensetivity for preceptation change than HBV model and the estimated mean annual soil moisture change by WASMOD model is higher than HBV estimated change for prceptation increasing scenarioes. For Elverum basin, WASMOD is more sensitive for preceptation change than HBV mode.

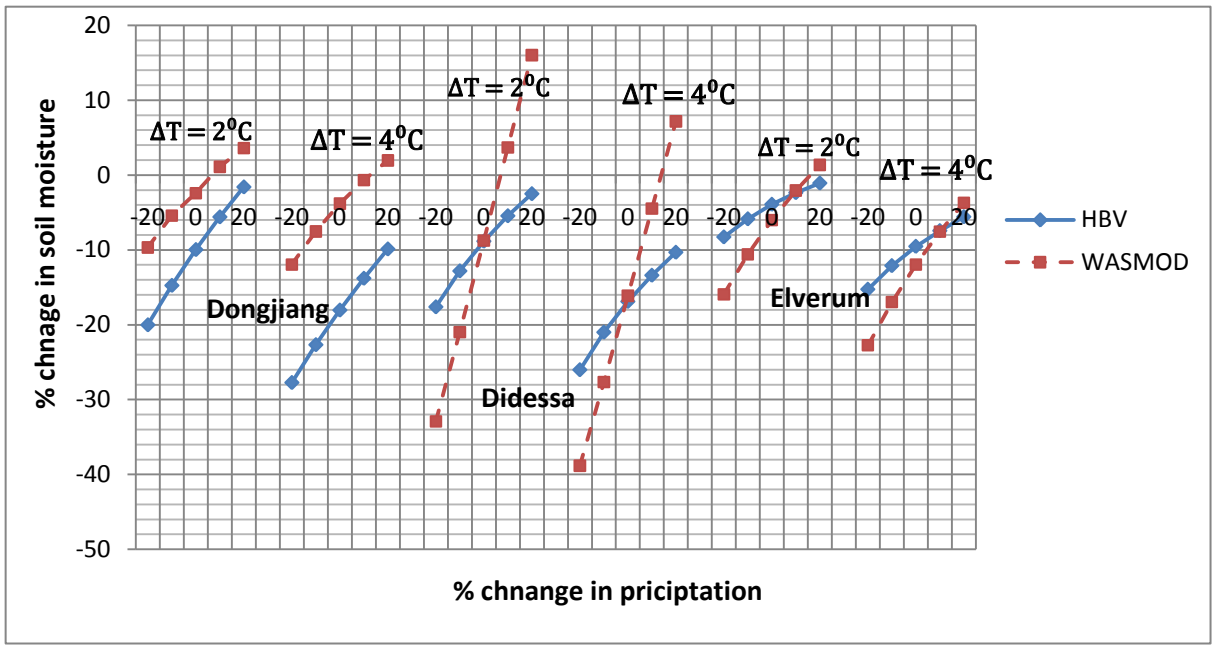

Figure 25. Comparison of mean annual change in soil moisture storage in response to precipitation increase for a given temperature change using WASMOD and HBV simulation for each basin

4.3.4 Sensitivity of the two models to estimate mean monthly runoff change

The estimation differences of mean monthly runoff by the two models for Elverum basin (For the increase in temperature from 2 ^{o}C to 4^{o}C combines with 20 % reduction and 20 % increase in precipitation) is shown in the Fig 26.

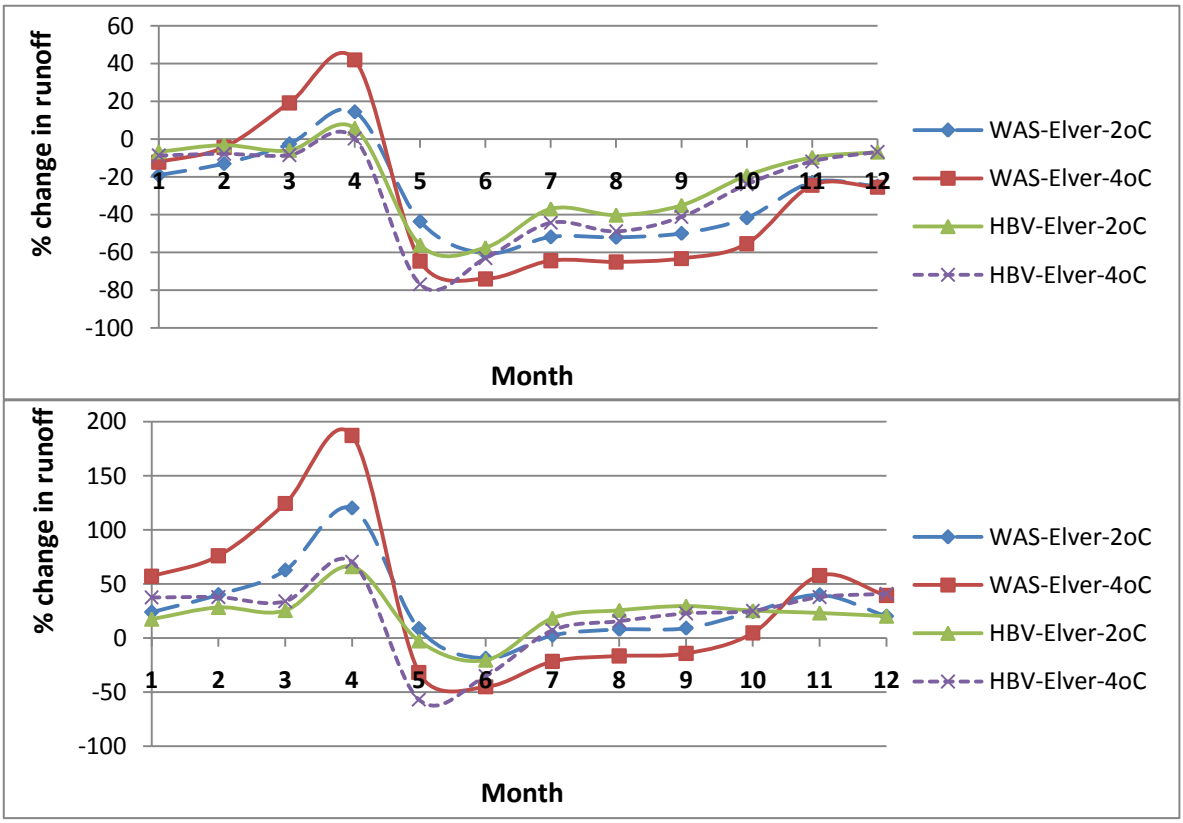

Figure 26 Comparison of mean monthly change in runoff in response to 20 % precipitation decrease (upper graph) and 20 % precipitation increase (lower graph) for a given temperature change using WASMOD and HBV simulation for Elverum basin

As it is revealed from the figure, the seasonal variability of runoff change estimated by both WASMOD and HBV models for Elverum basin has similar pattern. The runoff from late spring to early autumn (May to October), dropped considerably and the change is negative for both precipitation change scenario (ΔP = -20 %, in the upper graph and ΔP = +20 %, in the lower graph of Fig 26) by using both models. The prediction of change detected by HBV

model is relatively higher than the estimation of WASMOD during this period. At the same time the magnitudes of change in mean monthly runoff for a temperature increase by 2 ^{0}C and precipitation decrease by 20 % is relatively higher than the temperature change by 4 ^{0}C and precipitation increase by 20 % in both models case for this period.

During winter time (December to April) runoff increase in both model prediction and the magnitude of change is higher in WASMOD model prediction as compare with HBV model and relatively higher for 4^{0}C increases in temperature and 20% increase in precipitation, reflecting the fact that the temperature increases sufficiently enough to cause snowmelt and the combination of snowmelt with 20% precipitation increase results higher runoff during this time. The spring peak runoff is estimated in April using both models for both scenarios.

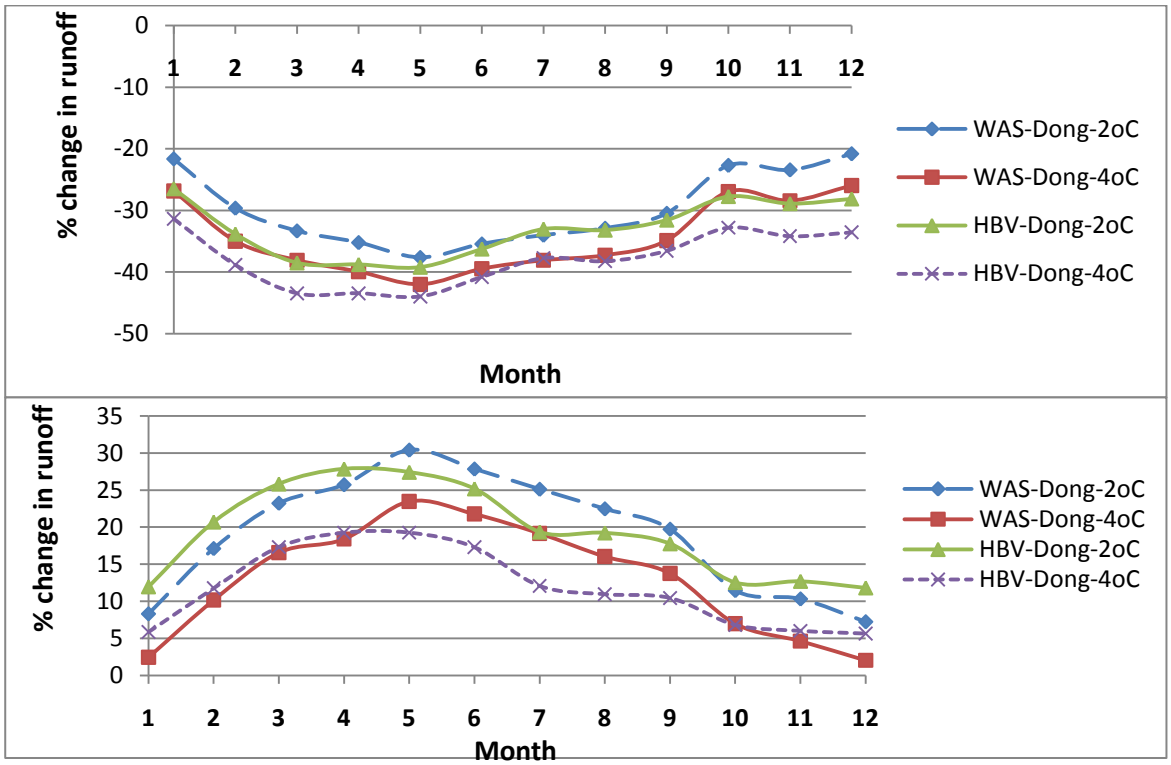

Figure 27. Comparison of mean monthly change in runoff in response to 20 % precipitation decrease (upper graph) and 20 % precipitation increase (lower graph) for a given temperature change using WASMOD and HBV simulation for Dongjiang basin

As it is illustrated in Fig 27, the estimation of mean monthly runoff at Dongjiang basin using WASMOD and HBV models have similar pattern for both scenario increases in temperature by 2 ^{0}C and 4 ^{0}C combine with 20 % reduction (upper graph) and 20 % increase (lower graph) in precipitation.

The estimation of mean monthly runoff by HBV model using the scenario of 20 % increase in precipitation (lower graph), is relatively higher from November to April as compare with WASMOD estimation. In both model runoff estimation, temperature increase from 2 ^{0}C to 4 ^{0}C for both precipitation change scenario results reduction in runoff.

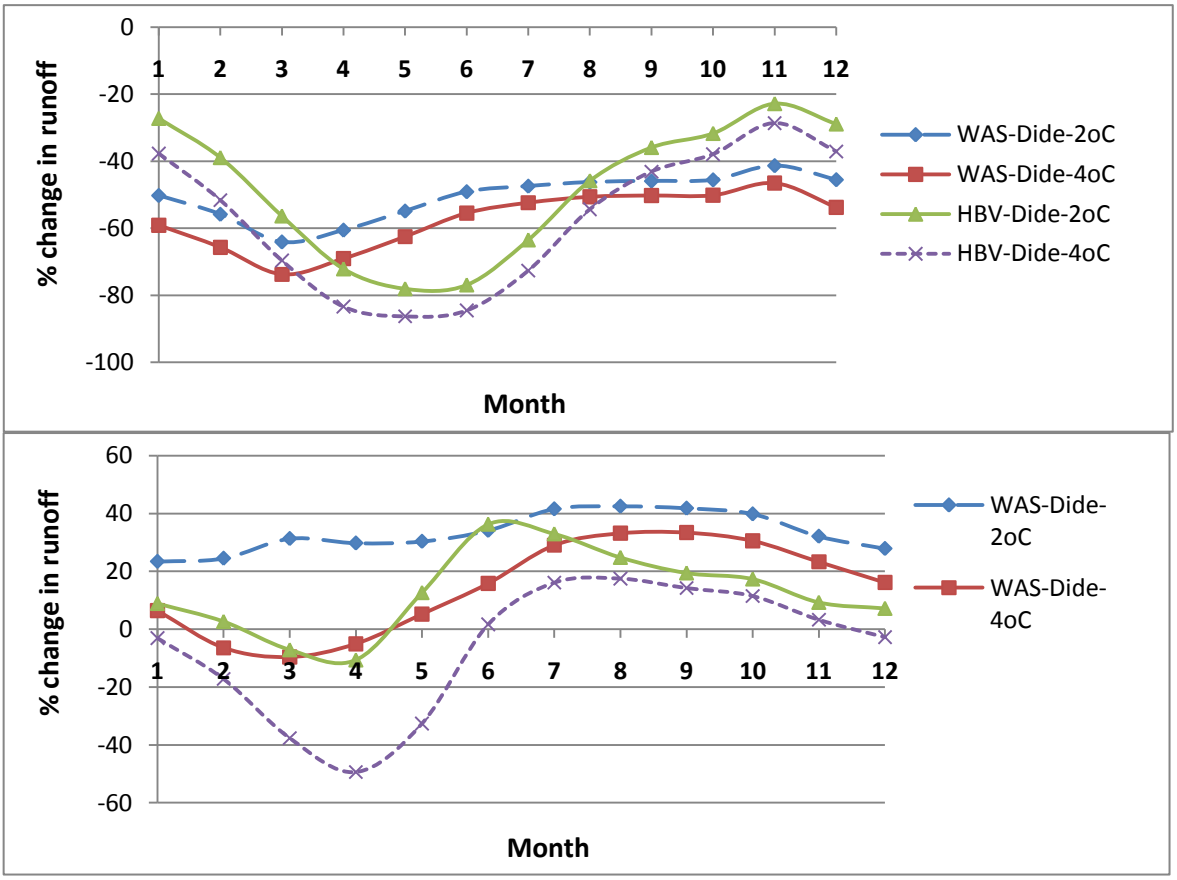

Figure 28 Comparison of mean monthly change in runoff in response to 20 % precipitation decrease (upper graph) and 20 % precipitation increase (lower graph) for a given temperature change using WASMOD and HBV simulation for Didessa basin

Fig 28 shows that the estimation of mean monthly runoff by using both WASMOD and HBV models has quite different pattern of seasonal variability for Didessa basin. For precipitation reduction scenario (ΔP = -20% in the upper graph), seasonal variability is lass in the case of WASMOD model estimation as compare with HBV model estimation. While significant reduction of runoff is estimated during rainy season by HBV model. On the other hand in the case of precipitation increase scenario (ΔP = +20% in the lower graph), the seasonal variability is higher in HBV prediction of runoff as compare with WASMOD prediction. In addition to this runoff reduction is estimated by WASMOD from February to April whereas HBV estimation shows more than 20 % runoff increase during this time.

4.3.5 Sensitivity of the two models to estimate mean monthly actual evapotranspiration change

Prediction difference of the two models on mean monthly actual evapotranspiration for Dongjiang basin using temperature increase from 2 ^{o}C to 4^{o}C and 20 % reduction and 20 % increase in precipitation scenarios is shown in Figure 29.

It shows that using precipitation reduction scenario (upper graph), estimation of actual evapotranspiration by using HBV model from March to July is relatively higher than the rest of months while in the estimation of WASMOD model, the estimation is relatively lower during this time. In the case of precipitation increase scenario (lower graph), the seasonal variation have similar patterns and the prediction of HBV model is relatively higher than WASMOD prediction.

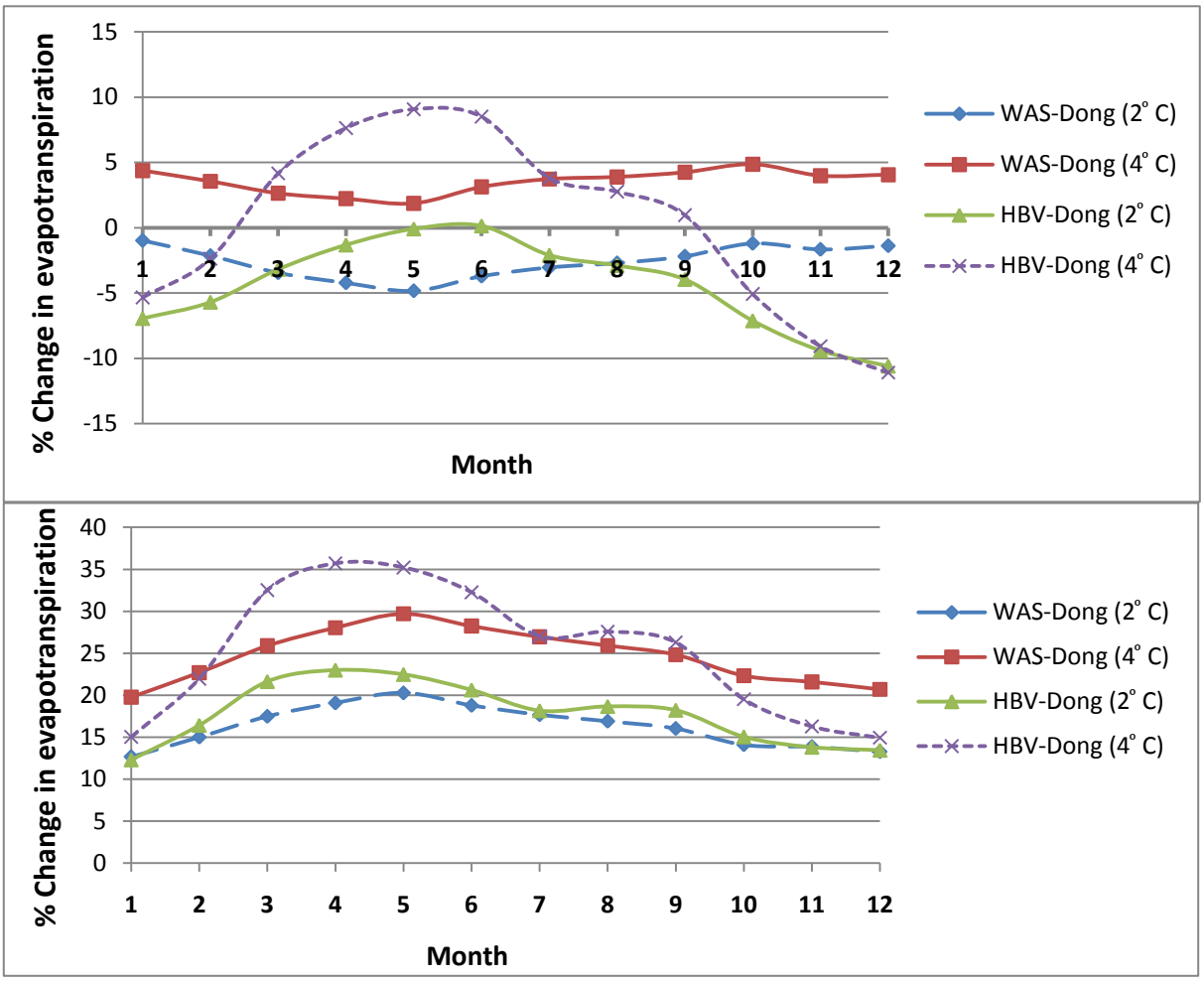

Figure 29 Comparison of mean monthly change in actual evapotranspiration in response to 20 % precipitation decrease (upper graph) and 20 % precipitation increase (lower graph) for a given temperature change using WASMOD and HBV simulation for Dongjiang basin.

Figure 30 Indicates that using scenario with precipitation reduced by 20 % (upper graph), the estimation of actual evaporation of the tow model for Didessa basin is considerably different during dry season (January to May) the change detected by HBV model is relatively higher than WASMOD estimation. Whereas during wet season, the two models detect the change similarly except HBV estimation using scenario with 4 ^{0}C temperature increase which detect the change relatively high. Using scenario with precipitation increase by 20 % (lower graph), the change detected by the two model is significantly varying from January to April during dry season for scenario with temperature increase by 2 ^{0}C. On the other hand from June to

December, the change estimated by WASMOD with 4^{o}C temprature increase scenario and by HBV with 2 ^{o}C temprature increase scenario is the same. Using scenario with 4 ^{0}C temperature increase, HBV model predicts much higher actual evapotranspiration change than WASMOD prediction for the same scenario during this period.

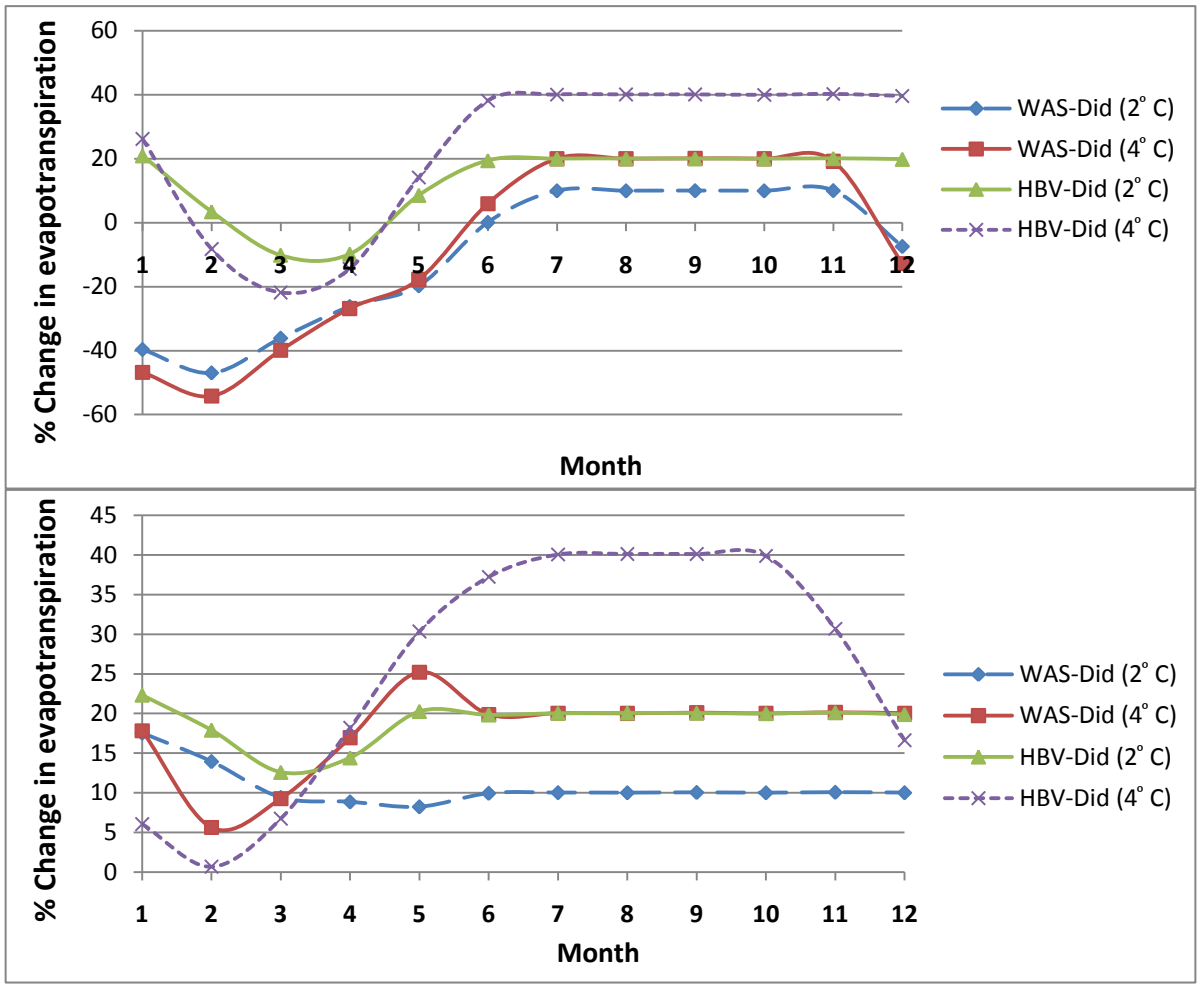

Figure 30 Comparison of mean monthly change in actual evapotranspiration in response to 20 % precipitation decrease (upper graph) and 20 % precipitation increase (lower graph) for a given temperature change using WASMOD and HBV simulation for Didessa basin.

The actual evapotranspiration change detected by the two model using scenario with precipitation reduced by 20 % (upper graph), for Elverum basin is shown in Fig 31. The pattern of seasonal variability detected by the two models is similar with significant magnitude difference. Using scenario with temperature change by 2^{0}C, the estimation of

WASMOD model is relatively higher during April and May and relatively lower from June to October as compared with HBV model prediction. The peak is in April according to WASMOD estimation whereas HBV estimation shows the peak in October. For scenario with temperature increase by 4^0C, HBV prediction is much higher than WASMOD prediction except April for which WASMOD estimates relatively higher.

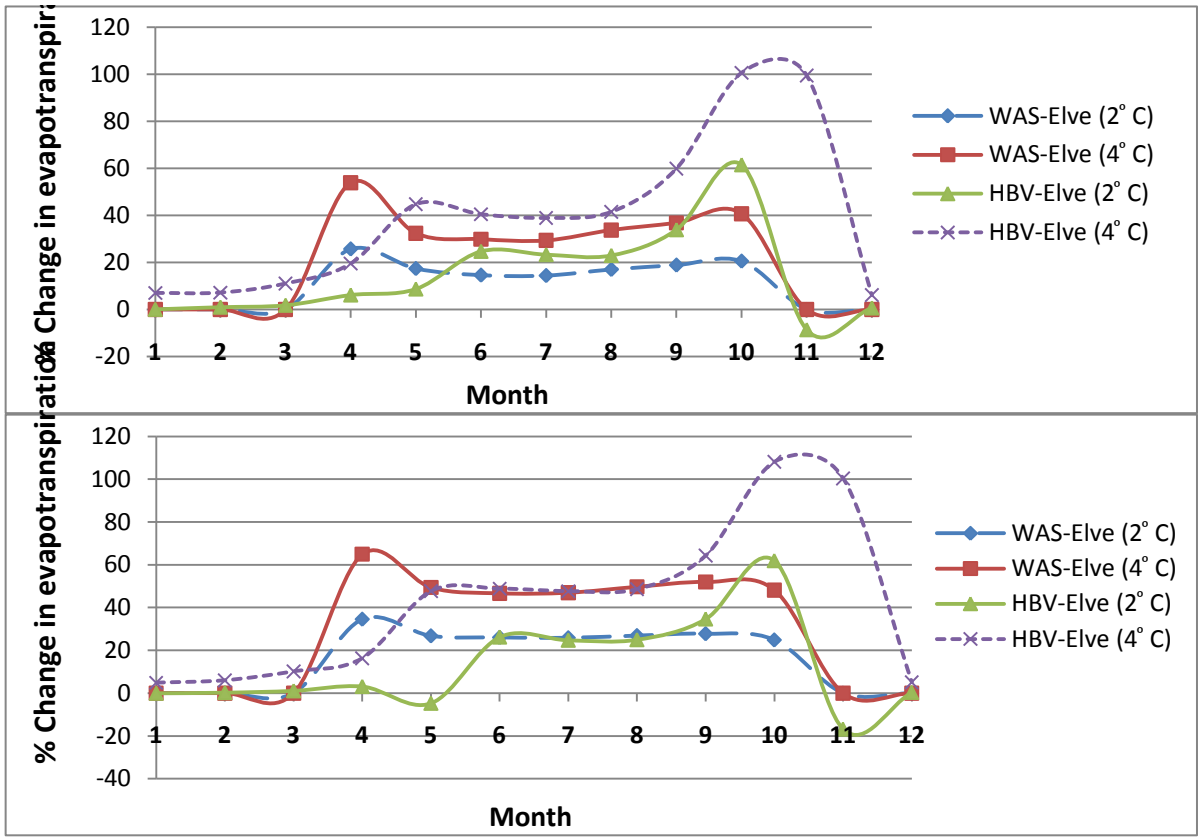

Figure 31 Comparison of mean monthly change in actual evapotranspiration in response to 20 % precipitation decrease (upper graph) and 20 % precipitation increase (lower graph) for a given temperature change using WASMOD and HBV simulation for Elverum basin

Using scenario with precipitation increase by 20 % (lower graph), the seasonal variability pattern is almost similar with the upper graph but the magnitude of change is relatively higher and the actual evapotranspiration change estimated by the two models for the months from June to August is almost the same.

4.3.6 Sensitivity of the two models to estimate mean monthly soil moisture storage change

The soil moisture change detected by the two models for Dongjiang basin is shown in Fig 32. As it indicated from the figure, soil moisture change detected by the two models using scenarios with precipitation reduced by 20 % (upper graph) and increase by 20 % (lower graph)is significantly different. Seasonal variability detected by WASMOD model is slightly higher than variability detected by HBV estimation for both scenarios. In addition to that, the magnitude of change estimated by HBV model is relatively lower as compare with the change detected by WASMOD model for both precipitation increase and reduction scenarios.

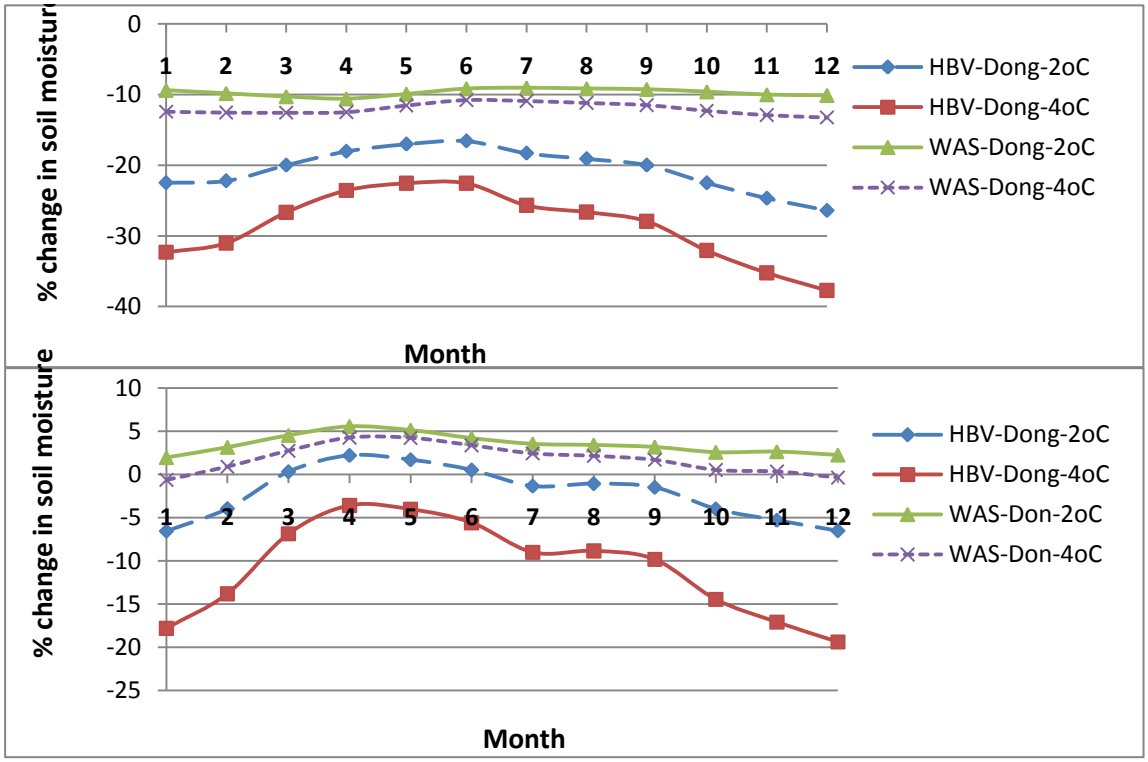

Figure 32 Comparison of mean monthly change in soil moisture storage in response to 20 % precipitation decrease (upper graph) and 20 % precipitation increase (lower graph) for a given temperature change using WASMOD and HBV simulation for Dongjiang basin.

The soil moisture change estimated by WASMOD and HBV models for Didessa basin is shown in Fig 33. The figure shows that, the patterns of seasonal variability detected by the two models are similar except magnitude differences for both scenarios. The change estimated by HBV model is relatively higher as compare with WASMOD model prediction for both scenarios. In the case of scenario with precipitation increase by 20 % and temperature increases by 2 ^{0}C, the change detected by WASMOD model is positive throughout the year and much higher than HBV model estimation for the same scenario.

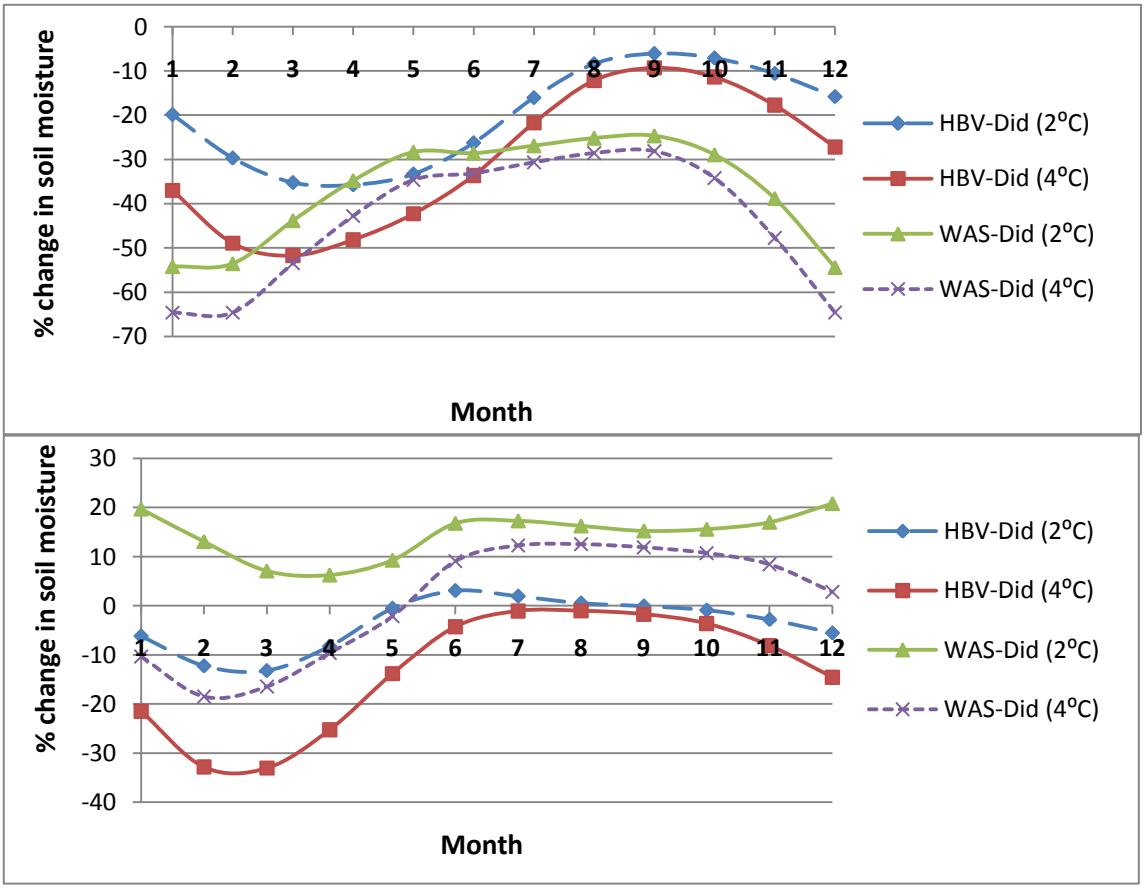

Figure 33 Comparison of mean monthly change in soil moisture storage in response to 20 % precipitation decrease (upper graph) and 20 % precipitation increase (lower graph) for a given temperature change using WASMOD and HBV simulation for Didessa basin.

As it is shown in Fig 34, seasonal variability of soil moisture storage change estimated by both models for Elverum basin has similar pattern. In the case of precipitation reduced by 20 % scenario, soil moisture storage change detected by HBV model is relatively lower as compared with WASMOD estimation and soil moisture storage change estimated for April is the same for both temperature change scenarios but HBV estimation of change is quite different. In the case of precipitation increase scenario (lower graph), the change detected by HBV model is lower as compared with WASMOD estimation of change.

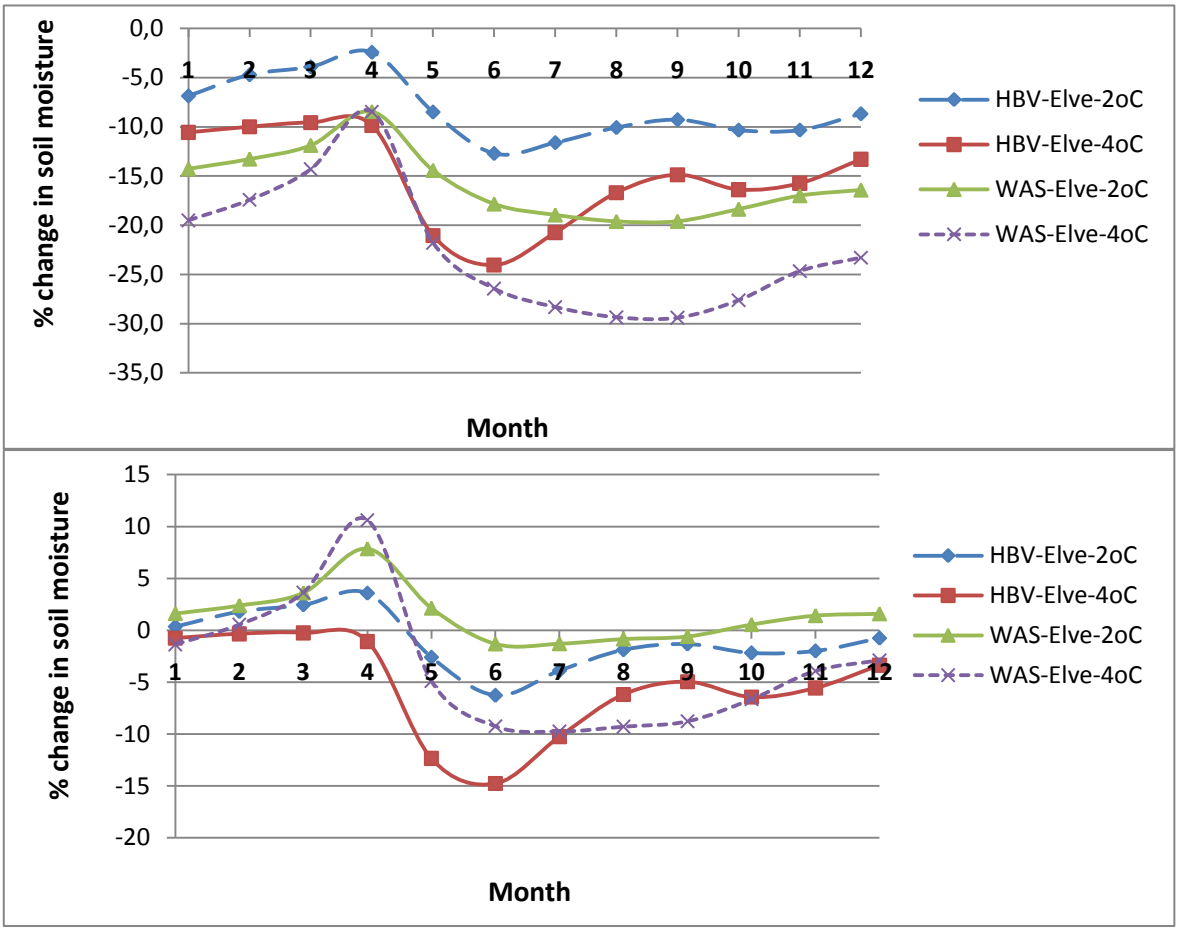

Figure 34 Comparison of mean monthly change in soil moisture storage in response to 20 % precipitation decrease (upper graph) and 20 % precipitation increase (lower graph) for a given temperature change using WASMOD and HBV simulation for Elverum basin.

5. Conclusion

In this study, WASMOD and HBV models were applied using different climate change scenarios to study the hydrological responses of climate change in Didessa, Dongjiang, and Elverum river basins located in different continents. The two models were preferred for their simplicity and flexibility in running with limited data set. The models can run using perception and temperature time series along with long term mean monthly evaporation and temperature data as inputs in the absence of other climatic data.

The calibration and validation results of WASMOD and HBV models were driven by observed hydro-climatic data set show that both models can reproduce the runoff with acceptable accuracy for each basin. One of the performance criterions which are used to evaluate the model result is Nash and Sutcliffe efficiency coefficient (E) and in this study it ranges from 0.88 to 0.94 for calibration and 0.80 to 0.90 for validation period using WASMOD model, and 0.88 to 0.96 during calibration and 0.84 to 0.95 during validation period using HBV model.

The hydrological impact of climate change resulted from synthetic scenario indicates that the sensitivity of catchments in response to different climate change scenario is quite different in different climatic regions. The mean annual runoff response was highly sensitive to precipitation and temperature changes in both models for Didessa and Elverum basins, respectively. However, mean annual runoff response to precipitation and temperature changes was moderately sensitive for Dongjiang basin. Actual evapotranspiration response to temperature change was highly sensitive in Elverum catchment, but less sensitive to precipitation change. Although Didessa show a higher sensitivity for precipitation change relative to Dongjiang, the actual evapotranspiration response to precipitation and

temperature was moderately sensitive in both models. The results imply that there is limitation in moisture and temperature for Didessa and Elverum respectively. WASMOD and HBV models show different Soil moisture storage response to precipitation change for all basins although the sensitivity was high for Didessa using WASMOD and low for Elverum in case of HBV model.

In terms of seasonal variability, there is high mean monthly runoff variation which is highly dependent on scenario, hydrological model, and the region where the catchment is found. Incremental scenario application for Dongjiang basin showed a very small seasonal variation for runoff in both model simulations. However, Elverum basin showed a considerable increase in late winter and early autumn runoff while spring runoff decreases in both model simulations except magnitude differences. For Didessa basin, there was significant difference between WASMOD and HBV simulations where the seasonal variation in runoff in the case of HBV simulation was high as compared with WASMOD simulation.

There are many sources of uncertainty in hydrological impact study using hydrological models. The result of this study demonstrates that model simulation under climate change condition is significantly different even though the performances of hydrological models are within the range of acceptable accuracy for a historical time series in a given environment.

Based on this finding, there is a concern that hydrological impact of climate change analysis using single hydrological model may lead to unreliable conclusion. In this regard, conducting multi model analysis is one way to reduce such uncertainty. Therefore, we recommend further research in this area in order to exhaustively explore hydrological impact of climate change in different regions.

References

Beldring, S., Engen-Skaugen, T., Forland, E.J. and Roald, L.A., 2008. Climate change impacts on hydrological processes in Norway based on two methods for transferring regional climate model results to meteorological station sites. Tellus Series a-Dynamic Meteorology and Oceanography, 60(3): 439-450.

Bergstrom, S. and Forsman, A., 1973. Development of a conceptual deterministic rainfall-runoff model. Nordic Hydrol, 4: 174–170.

Carter, T., M. Posch, and H. Tuomenvirta, 1995. SILMUSCEN and CLIGEN user's guide. Guidelines for the construction of climatic scenarios and use of a stochastic weather generator in the Finnish Research Programme on Climate Change (SILMU). Publications of the Academy of Finland, 1/95: 62.

Christensen, N.S., Wood, A.W., Voisin, N., Lettenmaier, D.P. and Palmer, R.N., 2004. The effects of climate change on the hydrology and water resources of the Colorado River basin. Climatic Change, 62(1-3): 337-363.

Conway, D., 2000. The climate and hydrology of the Upper Blue Nile river. Geographical Journal, 166: 49-62.

Donigian, A.S., 2005. Watershed Model Calibration and Validation:The HSPF experience, AQUA TERRA Consultants, Mountain View, CA 94043.

Dooge, J.C., 1977. Problems and methods of rainfall-runoff modelling. In: V.M.a.J.R.W. T.A. Ciriani (Editor), Mathematical models for surface water hydrology. John Wiley and Sons Ltd, London, England.

Engeland, K., Xu, C.Y. and Gottschalk, L., 2005. Assessing uncertainties in a conceptual water balance model using Bayesian methodology. Hydrological Sciences Journal-Journal Des Sciences Hydrologiques, 50(1): 45-63.

Gagnon, A.S. and Gough, W.A., 2005. Climate change scenarios for the Hudson Bay region: An intermodel comparison. Climatic Change, 69(2-3): 269-297.

Henny A.J. van Lanen, L.M.T., Miguel Candel, Jesus Carrera, Sue Crooks,, Kolbjørn Engeland, M.F., Ingjerd Haddeland, Hege Hisdal, Stanislav Horacek,, Jorge Jódar Bermúdez, A.F.v.L., Andrej Machlica, Vicente Navarro, and Prudhomme, O.N.C., 2008. Database with hydrometrological variables for selected river basins: Metadat catalogue, Water and Global Change (WATCH).

IPCC-TGICA, 2007. General Guidelines on the use of scenario data for climate impact and adaptation assessment, Intergovernmental Panel on Climate Change: Task Group on Data and Scenario Support for Impact and Climate Assessment (TGICA).

IPCC, 2001. IPCC 2001. Communication Dimensions. Proceedings IEEE International Professional Communication Conference (Cat. No.01CH37271). IPCC 2001. Communication Dimensions. Proceedings IEEE International Professional Communication Conference (Cat. No.01CH37271): xi+469.

IPCC, 2007. Climate Change 2007: Synthesis Report, Valencia, Spain.

Jha, M., Arnold, J.G., Gassman, P.W., Giorgi, F. and Gu, R.R., 2006. Climate change sensitivity assessment on Upper Mississippi River Basin streamflows using SWAT. Journal of the American Water Resources Association, 42(4): 997-1015.

Jiang, T. et al., 2007. Comparison of hydrological impacts of climate change simulated by six hydrological models in the Dongjiang Basin, South China. Journal of Hydrology, 336(3-4): 316-333.

Jin, X., Xu, C.-y., Zhang, Q. and Chen, Y.D., 2008. Regionalization study of a conceptual hydrological model in Dongjiang basin, south China. Quaternary International, In Press, Corrected Proof.

Jothityangkoon, C., Sivapalan, M. and Farmer, D.L., 2001. Process controls of water balance variability in a large semi-arid catchment: downward approach to hydrological model development. Journal of Hydrology, 254(1-4): 174-198.

Karl, T.R., 1996. The IPCC (1995) scientific assessment of climate change: Observed climate variability and change. Seventh Symposium on Global Change Studies: 7-13.

Seibert, J., 1997. Estimation of parameter uncertainty in the HBV model. Nordic Hydrology, 28(4-5): 247-262.

Seibert, J., 2005. HBV light User's Manual. Uppsala University, Department of Earth Sciences, Hydrology, Uppsala, pp. 3-16.

Seibert. J., 1998. HBV light User's Manual. Uppsala University, Department of Earth Sciences, Hydrology, Uppsala, 3-16 pp.

Seino, H., Kai, K., Ohta, S., Kanno, H. and Yamakawa, S., 1998. Concerning the IPCC report (1996): General remarks of research group for impacts of climate change (ICC). Journal of Agricultural Meteorology, 54(2): 179-186.

Steele-Dunne, S. et al., 2008. The impacts of climate change on hydrology in Ireland. Journal of Hydrology, 356(1-2): 28-45.

Xu, C.-Y., 2002. WASMOD - The Water And Snow balance MODelling system. In: V.P.a.F. Singh, D. K. (Editor), Mathematical Models of Small Watershed Hydrology and Applications. Water Resources Publications, Colorado, USA., pp. 443-476.

Xu, C.Y., 1999. Climate change and hydrologic models: A review of existing gaps and recent research developments. Water Resources Management, 13(5): 369-382.

Xu, C.Y., 2000. Modelling the effects of climate change on water resources in central Sweden. Water Resources Management, 14(3): 177-189.

Xu, C.Y., 2006. Runoff Modelling: Hydrological Models University of Oslo, Environmental Geology Hydrology and Geohazards, pp. 200.

Xu, C.Y., Widen, E., and Halldin, S., 2005. Modelling Hydrological Consequences of Climate Change – Progress and Challenges. Advances in Atmospheric Sciences, 22(6): 787-797.

Appendices

Appendix 1 Simulated and observed monthly runoff for each catchment using WASMOD model

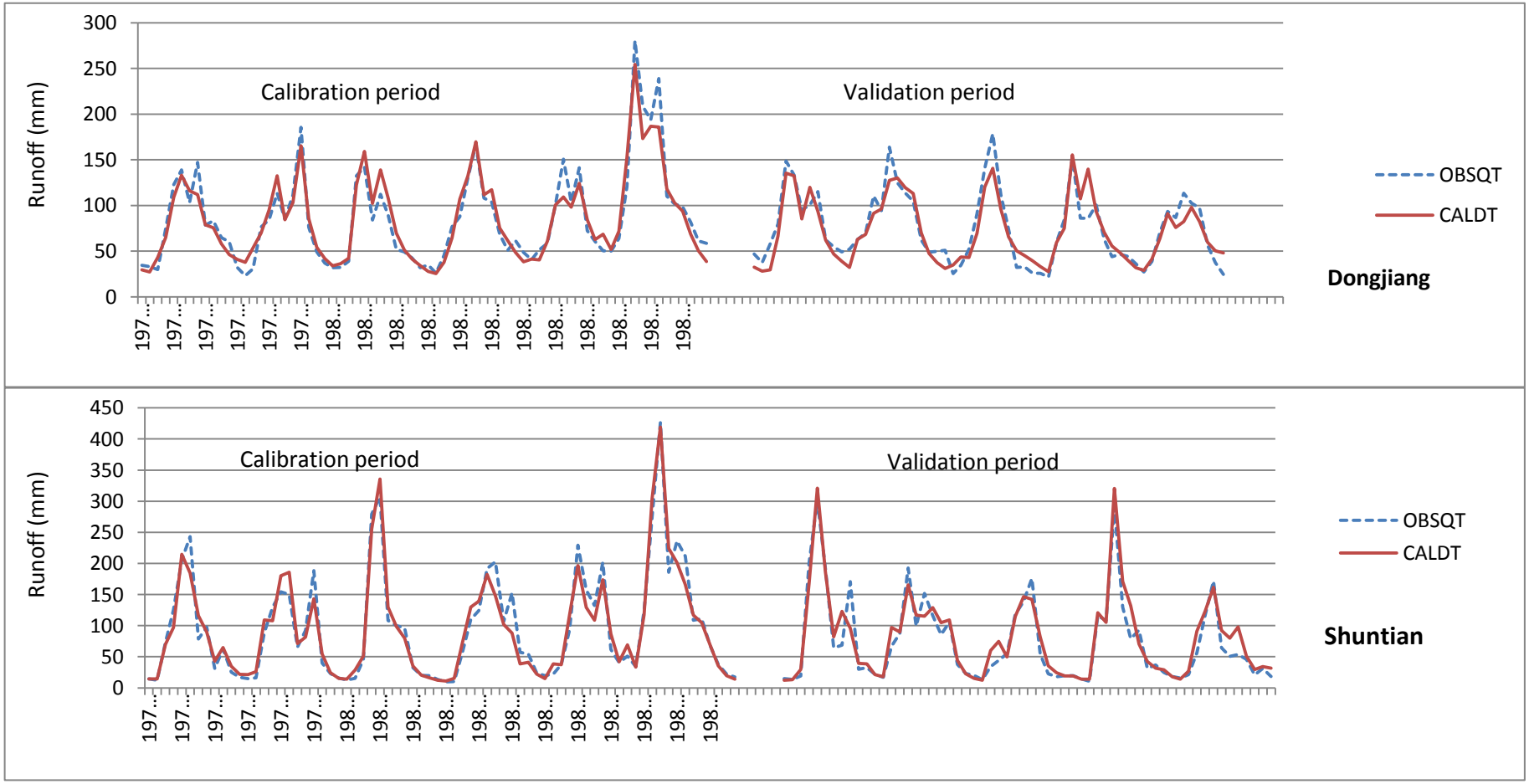

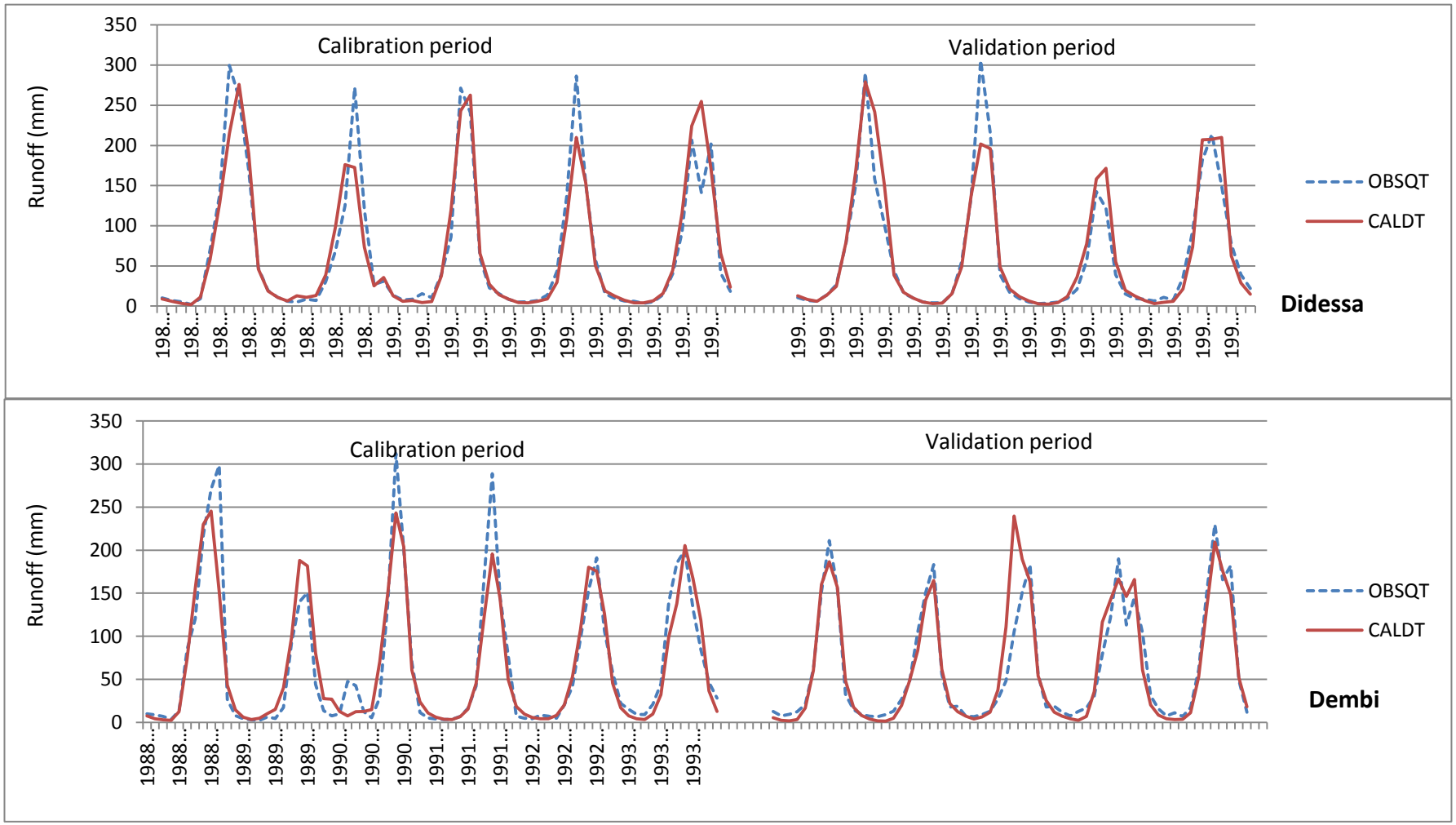
Calibration period
Validation period
Runoff (mm)
350
300
250
200
150
100
50
0
OBSQT
CALDT
Didessa
Calibration period
Validation period
Runoff (mm)
OBSQT
CALDT
Dembi

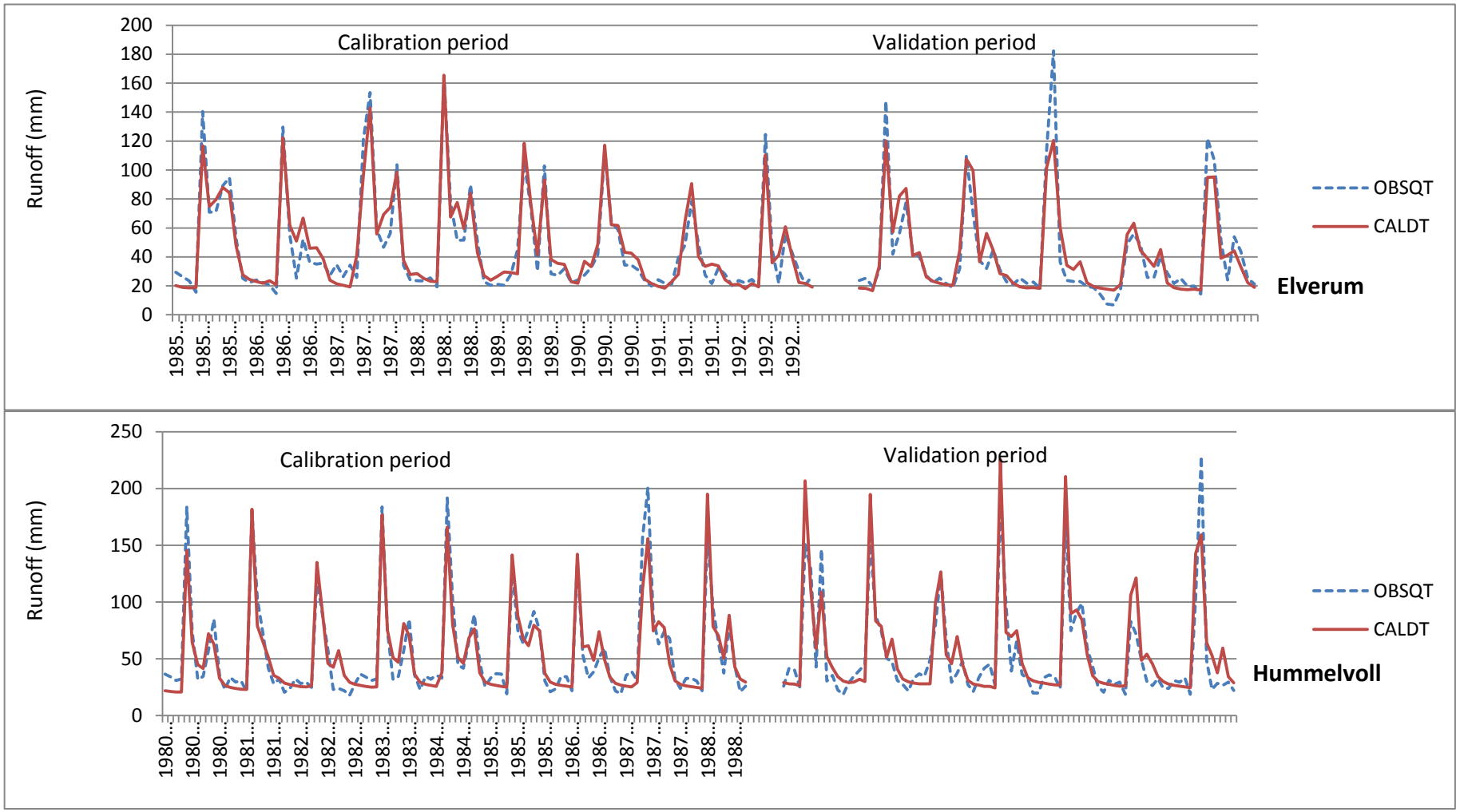

Appendix 2 Simulated and observed monthly runoff for each catchment using HBV model

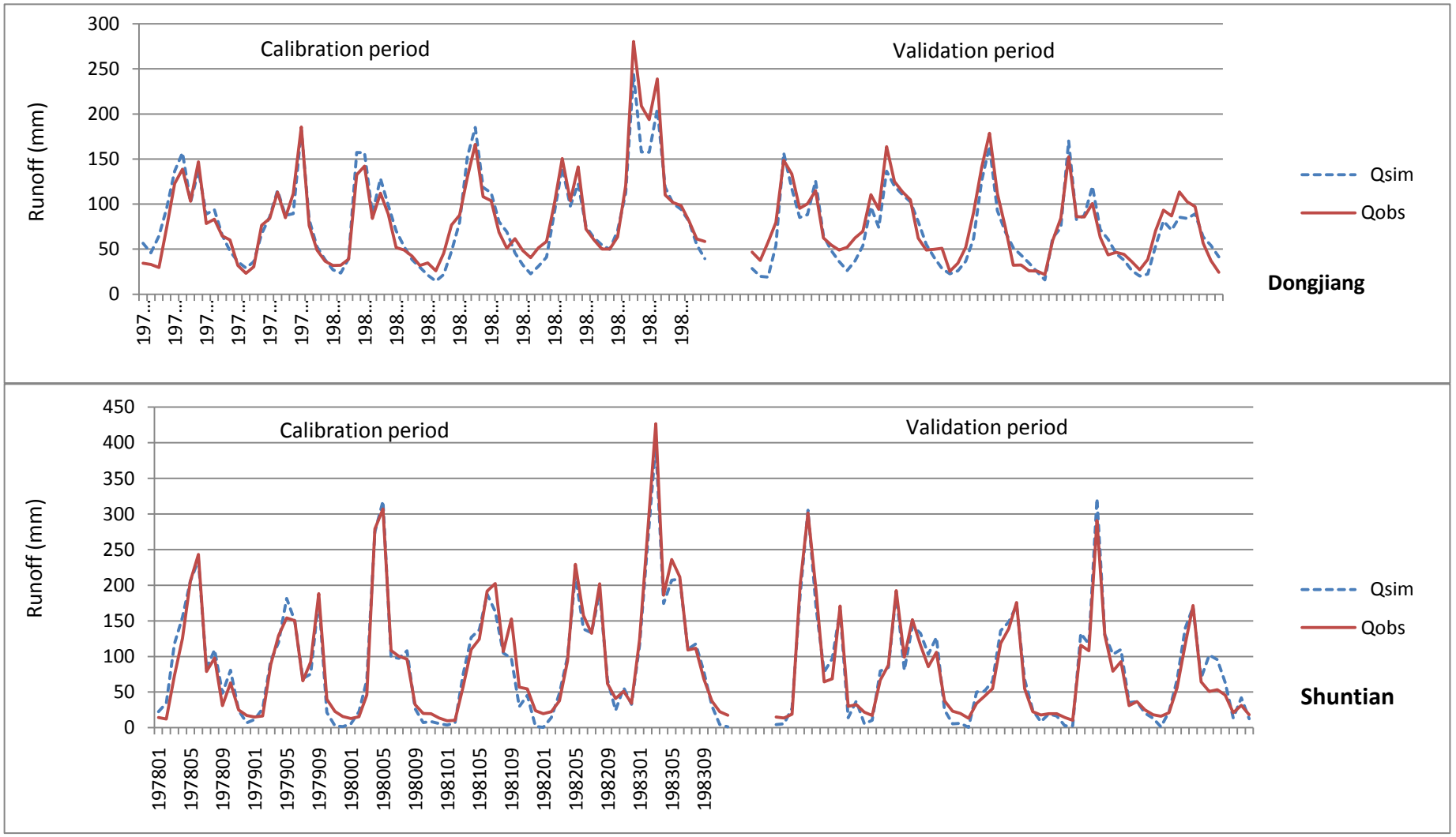
Runoff (mm)
Calibration period
Validation period
Qsim
Qobs
Dongjiang
Runoff (mm)
Calibration period
Validation period
Qsim
Qobs
Shuntian

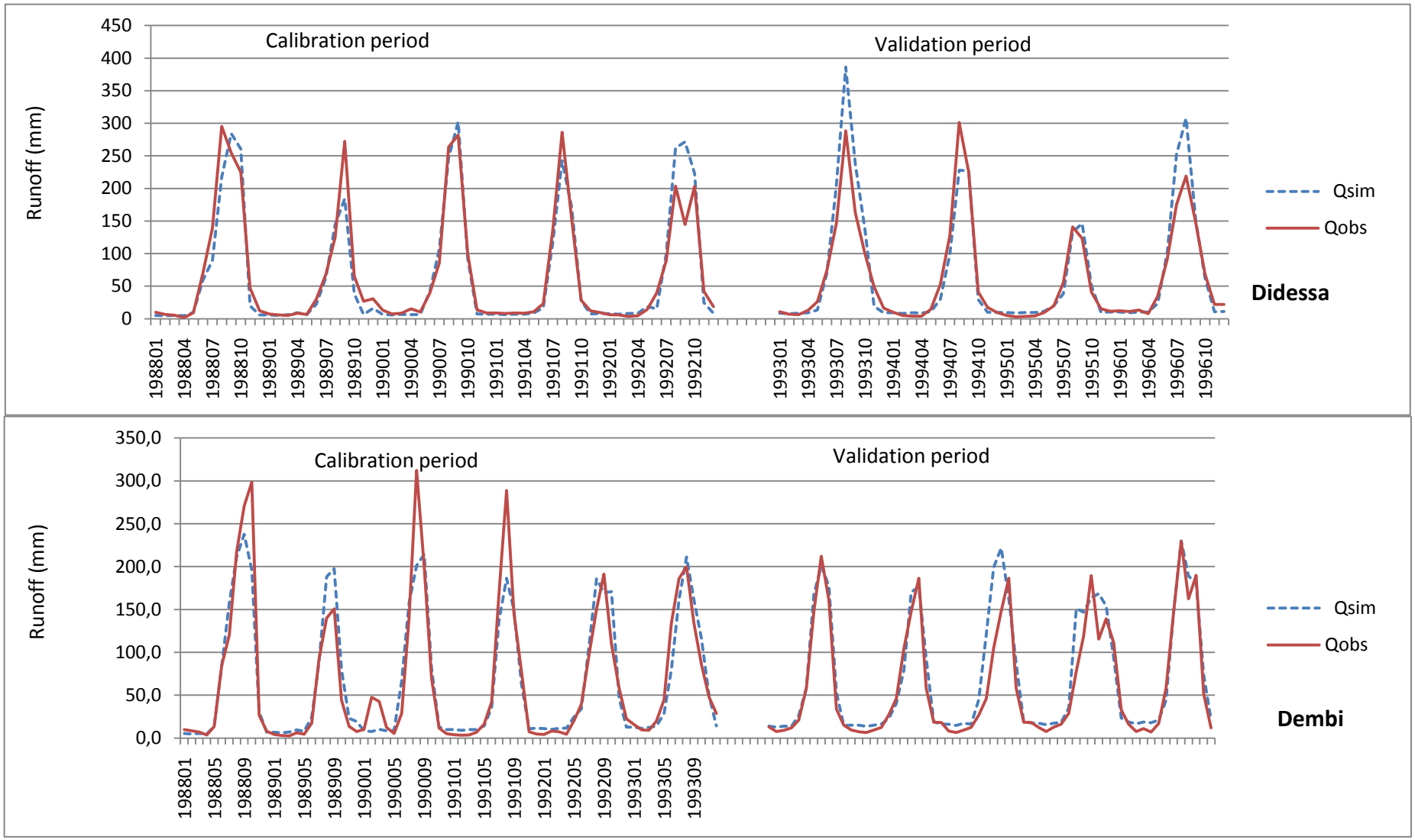
Runoff (mm)
Calibration period
Validation period
Qsim
Qobs
Didessa
Runoff (mm)
Calibration period
Validation period
Qsim
Qobs
Dembi

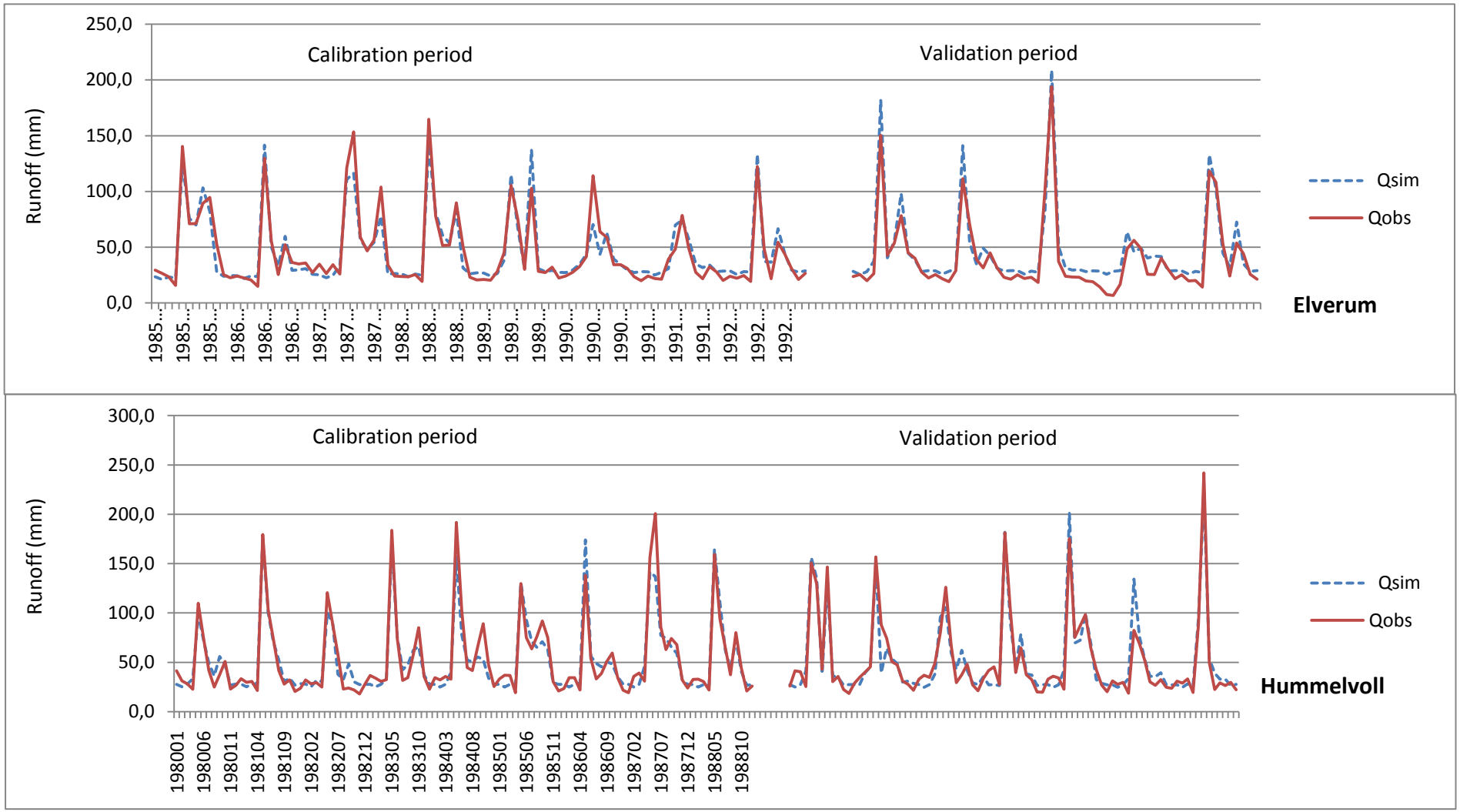
Runoff (mm)
250,0
200,0
150,0
100,0
50,0
0,0
Calibration period
Validation period
Qsim
Qobs
Elverum
1985...
1985...
1985...
1986...
1986...
1986...
1987...
1987...
1987...
1988...
1988...
1988...
1989...
1989...
1989...
1990...
1990...
1990...
1991...
1991...
1991...
1992...
1992...
1992...
Runoff (mm)
300,0
250,0
200,0
150,0
100,0
50,0
0,0
Calibration period
Validation period
Qsim
Qobs
Hummelvoll
198001
198006
198011
198104
198109
198202
198207
198212
198305
198310
198403
198408
198501
198506
198511
198604
198609
198702
198707
198712
198805
198810